JOC The Journal of Organic Chemistry



Article

# Total Synthesis and Biological Mode of Action of WAP-8294A2: A Menaquinone-Targeting Antibiotic

Hiroaki Itoh, Kotaro Tokumoto, Takuya Kaji, Atmika Paudel, Suresh Panthee, Hiroshi Hamamoto, Kazuhisa Sekimizu, and Masayuki Inoue

*J. Org. Chem.*, **Just Accepted Manuscript** • DOI: 10.1021/acs.joc.7b02318 • Publication Date (Web): 11 Oct 2017



## Just Accepted



ACS Publications

The Journal of Organic Chemistry is published by the American Chemical Society. 1155 Sixteenth Street N.W., Washington, DC 20036

# Total Synthesis and Biological Mode of Action of WAP-8294A2: A Menaquinone-Targeting Antibiotic

Hiroaki Itoh,[†] Kotaro Tokumoto,[†] Takuya Kaji,[†] Atmika Paudel,[‡] Suresh Panthee,[‡] Hiroshi Hamamoto,[‡] Kazuhisa Sekimizu,[‡] and Masayuki Inoue*[†]

[†]*Graduate School of Pharmaceutical Sciences, The University of Tokyo, 7-3-1 Hongo, Bunkyo-ku, Tokyo 113-0033, Japan.*

[‡]*Teikyo University Institute of Medical Mycology, 359 Otsuka, Hachioji, Tokyo 192-0395, Japan.*

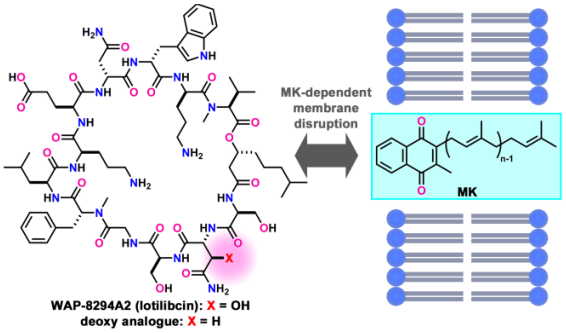


**ABSTRACT:** WAP-8294A2 (lotilibcin, **1**) is a potent antibiotic with superior *in vivo* efficacy to vancomycin against methicillin-resistant *Staphylococcus aureus* (MRSA). Despite the great medical importance, its molecular mode of action remains unknown. Here we report the total synthesis of complex macrocyclic peptide **1** comprised of 12 amino acids with a *β*-hydroxy fatty-acid chain, and its deoxy analogue **2**. A full solid-phase synthesis of **1** and **2** enabled their rapid assembly and the first detailed investigation of their functions. Compounds **1** and **2** were equipotent against various strains of Gram-positive bacteria including MRSA. We present evidence that the antimicrobial activities of **1** and **2** are due to lysis of the bacterial membrane, and their membrane-disrupting effects depend on the presence of menaquinone, an essential factor for the bacterial respiratory chain. The established synthetic routes and the menaquinone-targeting mechanisms provide valuable information for designing and developing new antibiotics based on their structures.

## INTRODUCTION

Antibiotics are crucial in modern medicine for the treatment of infectious diseases and invasive surgery, and their use has increased life expectancy. The number of infections caused by multidrug-resistant bacteria is increasingly globally, however, and nosocomial infections caused by methicillin-resistant *Staphylococcus aureus* (MRSA) in hospitals have become an especially serious clinical problem.[1,2] Therefore, antibiotics that belong to new structural classes and manifest their biological activity via novel mechanisms are urgently needed.[3,4,5,6]

Among the underutilized antibiotic candidate groups, cyclic peptides represent a promising class of natural products with potent antibacterial activity.[7,8,9,10] In 1997, WAP-8294A2 (**1**, Figure 1), which is also known as lotilibcin, was isolated from a culture broth of *Lysobacter* sp. strain, and structurally determined to be an antimicrobial cyclic depsipeptide.[11,12,13,14,15] The antibiotic **1** has potent bactericidal activity against otherwise antibiotic-resistant Gram-positive pathogens, including methicillin-resistant *S. aureus* (MRSA) clinical isolates (minimum inhibitory concentration [MIC] = 0.78 μg/mL). Assessment of the *in vivo* efficacy of **1** in an experimental systemic MRSA mouse infection model revealed that **1** is 10 times more active than vancomycin, which is a last line of resort in treating MRSA infections (median effective dose [$ED_{50}$] of **1** = 0.38 mg/kg; $ED_{50}$ of vancomycin = 5.3 mg/kg). Consequently, **1** is considered a promising lead structure for the development of new antibiotics against multidrug-resistant human pathogenic bacteria, and has entered phase I clinical trials against systemic MRSA infection.[16]

Despite the medical importance of **1**, its antibacterial mechanism has not been investigated in detail, and its chemical synthesis has only been recorded in a PhD thesis.[17] In 1998, the antimicrobial activity of **1** was reportedly decreased by addition of the typical negatively-charged lipids of bacterial membranes, phosphatidylglycerol (PG) and cardiolipin (CL).[12] Because the net charge of **1** is positive, the antagonistic activities of PG and CL are likely due to non-specific electrostatic effects rather than a specific

interaction of **1** with the anionic lipids. Accordingly, the molecular target of **1** remains to be clarified.

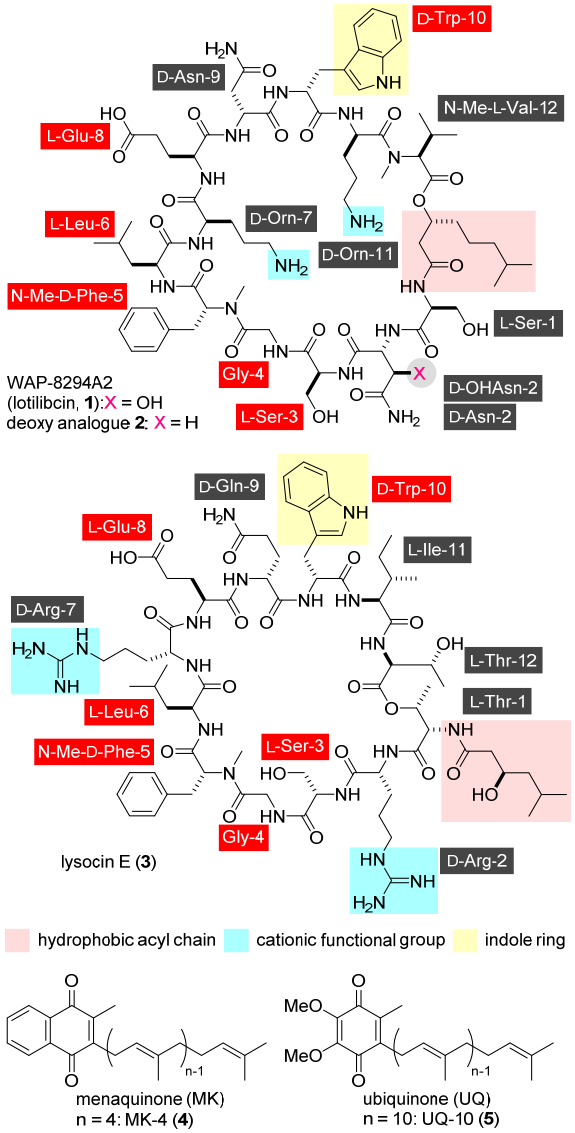


**Figure 1.** Structures of WAP-8294A2 (lotilibcin, **1**), deoxy analogue **2**, lysocin E (**3**), menaquinone-4 (MK-4, **4**), and ubiquinone-10 (UQ-10, **5**). Amino acids common to **1** and **3** are highlighted in red. Other amino acids are highlighted in dark grey. The hydrophobic acyl chains, cationic functional groups, and indole moieties of **1** and **3** are highlighted in pink, cyan, and yellow, respectively.

Structurally, **1** has a 40-membered macrocycle comprising (*R*)-3-hydroxy-7-methyloctanoic acid and 12 amino acid residues with an ester linkage (Figure 1). There are five proteinogenic (L-Ser-1, L-Ser-3, Gly-4, L-Leu-6, L-Glu-8) and seven non-proteinogenic amino acid residues (D-OHAsn-2, N-Me-D-Phe-5, D-Orn-7, D-Asn-9, D-Trp-10, D-Orn-11, N-Me-L-Val-12) within the sequence. By close inspection of the structure of **1**, we identified striking structural similarity between **1** and the antibiotic lysocin E (**3**), although the sizes of their macrocycles differ (40- vs. 37-membered).[18,19] Six amino acid residues (colored in red) are shared by the sequences of **1** and **3** (L-Ser-3, Gly-4, N-Me-D-Phe-5, L-Leu-6, L-Glu-8, and D-Trp-10). Moreover, **1** and **3** have a hydrophobic acyl chain at L-Ser-1 and L-Thr-1, respectively, and two cationic groups at D-Orn-7/11 and D-Arg-2/7, respectively. The analogous patterns of the functional groups of **1** and **3** raised the possibility that these two peptides have related mechanisms of action.

The mode of action of **3** has been shown to be distinct from those of any other reported antibiotics.[18] The molecular target of **3** is menaquinone (MK), which is an essential factor for electron transfer in the bacterial respiratory chain.[20,21] While **3** forms a 1:1 complex with MK ($K_D$ = 4.5 μM), no apparent complexation occurs between **3** and ubiquinone (UQ), a coenzyme in the mammalian respiratory chain. Formation of the **3**-MK complex is considered to disrupt the membrane integrity of bacterial cells in the presence of mammalian cells, resulting in rapid and selective bacteriolysis. This intriguing function of **3** motivated us to conduct solid-phase total synthesis and comprehensive structure-activity relationship (SAR) studies of **3** in 2015[22] and 2016,[23] respectively. As a result, we established the biologically important functionalities of **3** to be the cationic functional groups at D-Arg-2/7 (highlighted in cyan), the hydrophobic acyl chain at L-Thr-1 (pink), and the indole ring at D-Trp-10 (yellow). Since **1** possesses all of these characteristic features of **3**, we hypothesized that **1** also displays antibacterial activity by targeting MK.

In this manuscript, we first report the full solid-phase total synthesis of WAP-8294A2 (**1**) as well as its more synthetically accessible deoxy analogue **2**. Rapid and efficient synthetic preparation of **1** and **2** allowed us to perform a series of detailed functional analyses. Consequently, we corroborated that **1** and **2** indeed exert their antimicrobial activities by MK-dependent membrane lysis. These findings decipher the molecular mode of action of **1** for the first time.

## RESULTS AND DISCUSSION

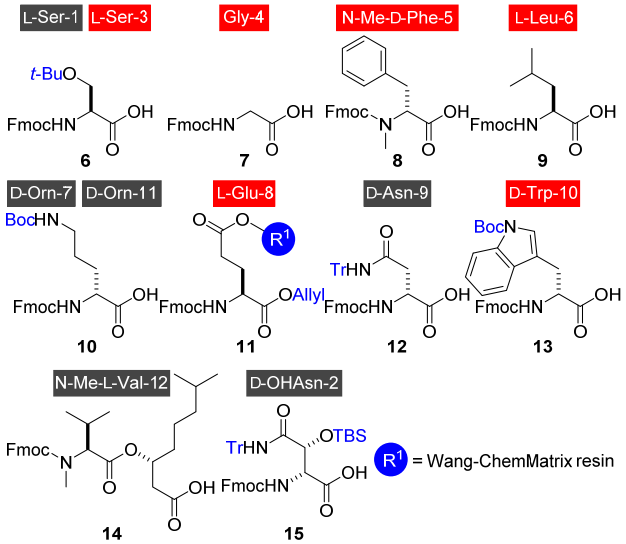


**Figure 2.** Building blocks for **1** and **2**. Boc = *tert*-butoxycarbonyl; Fmoc = 9-fluorenylmethoxycarbonyl; TBS =

*tert*-butyldimethylsilyl; *t*-Bu = *tert*-butyl; Tr = triphenylmethyl.

**Scheme 1. Synthesis of 14 and 15**[a]

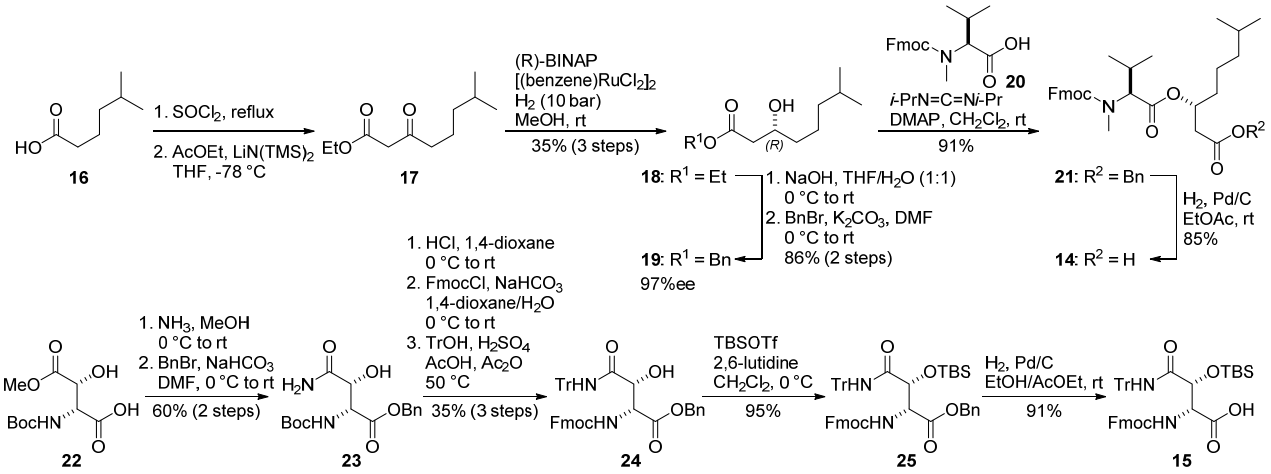


[a]BINAP = 2,2'-bis(diphenylphosphino)-1,1'-binaphthyl; DMAP = 4-(*N*,*N*-dimethylamino)pyridine; $LiN(TMS)_2$ = lithium bis(trimethylsilyl)amide.

**Synthetic strategy.** We adopted a full solid-phase strategy for the total synthesis of WAP-8294A2 (**1**) because it omits multiple chromatographic purifications and ensures rapid preparation of a wider variation of analogues for future SAR studies compared with the solution-phase counterpart. Accordingly, the structure of **1** was retrosynthetically disassembled into 10 different building blocks **6**-**15** (Figure 2). Fmoc-based solid-phase peptide synthesis (SPPS) was planned to be applied beginning with **11**,[24,25] the side-chain of which was anchored to Wang-ChemMatrix resin.[26] The ester linkage between N-Me-L-Val-12 and (*R*)-3-hydroxy-7-methyloctanoic acid was envisioned to be preformed as **14** to avoid inefficient ester condensation on the solid matrices. The full solid-phase strategy would therefore involve the following sequential operations:[22,23,27,28,29,30,31] (1) stepwise solid-phase assembly of the linear dodecapeptide from **11**; (2) chemoselective removal of the allyl group of L-Glu-8 under palladium-catalyzed neutral conditions; (3) intramolecular amidation between the $C_\alpha$-carboxyl group of L-Glu-8 and the $N_\alpha$-amino group of D-Asn-9, taking advantage of the pseudo-dilution phenomenon that favors intramolecular reactions of the resin-bound molecules;[32,33] and (4) trifluoroacetic acid (TFA) treatment for simultaneous cleavage from the Wang-ChemMatrix resin and global deprotection of the acid-labile side-chain protective groups (TBS, Boc, and Tr) to release **1**. While $N_\alpha$-Fmoc-protected amino acids **6**-**13** were commercially available, ester **14** and TBS-protected D-OHAsn-2 **15** required synthetic preparation.[34,35,36] Another target molecule, deoxy WAP-8294A2 (**2**), was designed as a more synthetically accessible analogue of **1**, because **12** would be used instead of **15** as a common building block for both D-Asn-2 and D-Asn-9. From a biological perspective, it would be more useful if the activity assays of synthesized **1** and **2** shed light on the importance of the *β*-hydroxy group of D-OHAsn-2.[37,38]

**Preparation of building blocks 14 and 15.** The synthesis of ester **14** started from 5-methylhexanoic acid **16** (Scheme 1). After **16** was subjected to thionyl chloride, the resultant acid chloride was treated with ester enolate generated from AcOEt and $LiN(TMS)_2$, resulting in the formation of β-keto ester **17**. Asymmetric Noyori hydrogenation of **17** using $RuCl_2$[(*R*)-BINAP] as the catalyst gave rise to **18**.[39] Hydrolysis of ethyl ester **18** by aqueous NaOH and subsequent protection of the carboxylic acid as the benzyl ester generated benzyl (*R*)-3-hydroxy-7-methyloctanoate **19**. The enantiomeric excess of **19** was determined to be 97% by chiral HPLC analysis (Figure S1). Secondary alcohol **19** and Fmoc-N-Me-L-Val-OH **20** were then condensed by the action of diisopropylcarbodiimide and DMAP, leading to **21**. Finally, hydrogenolysis in the presence of Pd/C under $H_2$ atmosphere transformed the benzyl ester of **21** to the carboxylic acid of **14**.

Compound **15** was prepared from the known D-aspartate derivative **22**.[40] Ester-amide exchange reaction of **22** using $NH_3$ was followed by treatment with BnBr and $NaHCO_3$ to provide **23**.[41,42] Then, three-step protective group manipulations from **23** furnished $N_\alpha$-Fmoc-, $C_\alpha$-$CO_2$Bn-, and $C_\gamma$N-Tr-protected *β*-hydroxy D-asparagine **24**. The secondary hydroxy group of **24** was protected as its TBS ether using TBSOTf and 2,6-lutidine to generate **25**. The benzyl group of **25** was in turn removed by applying $H_2$ and Pd/C, giving rise to the requisite **15** with the appropriate protective groups for the next SPPS.

**Solid-phase total synthesis of WAP-8294A2 (1) and deoxy analogue 2.** The SPPS of **1** and **2** started from allyl glutamate-loaded resin **11** (Scheme 2). First, $N_\alpha$-Fmoc of **11** was removed by treatment with 20% piperidine/NMP to give a free amine. The peptide chains of **1** and **2** were elongated at 40 °C under microwave-assisted conditions to facilitate the condensation.[43,44] Cycles of 20% piperidine/NMP-promoted $N_\alpha$-deprotection (10 min, rt) and

**Scheme 2. Solid-phase total syntheses of 1 and 2**[a]

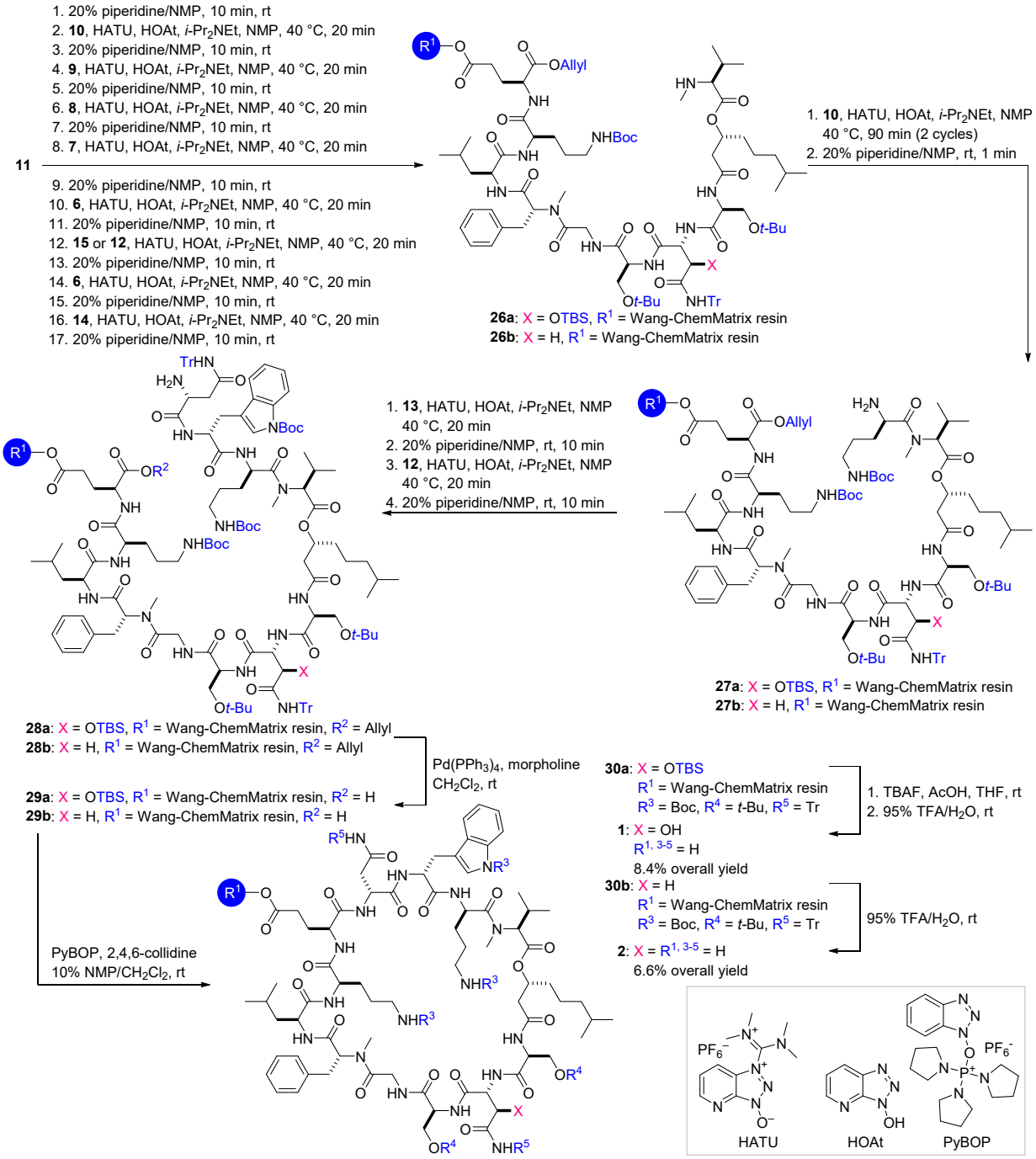


[a]HATU = *O*-(7-aza-1H-benzotriazol-1-yl)-*N*,*N*,*N*′,*N*′-tetramethyluronium hexafluorophosphate; HOAt = 1-hydroxy-7-azabenzotriazole; NMP = *N*-methyl-2-pyrrolidone; PyBOP = (benzotriazol-1-yloxy)tripyrrolidinophosphonium hexafluorophosphate; TBAF = tetrabutylammonium fluoride; TFA = trifluoroacetic acid.

HATU/HOAt[45]-mediated amide coupling (20 min, 40 °C) were applied to **11** using **10**, **9**, **8**, **7**, **6**, **15** for **1** or **12** for **2**, **6**, and **14**. These repeated reactions resulted in the formation of the resin-bound nonapeptide **26a**/**b** including the ester linkage after removal of the Fmoc group at the N-terminus under basic conditions. The next reaction of **10** with the sterically demanding N-methyl amine of **26a**/**b** necessitated a double coupling sequence with a longer reaction time (90 min). Then, the piperidine treatment for the subsequent $N_\alpha$-deprotection was shortened to 1 min to prevent diketopiperazine formation via attack of the N-terminal amine of D-Orn-11 of **27a**/**b** to the proximal ester carbonyl group. The thus obtained decapeptide **27a**/**b** was again subjected to two cycles of

the condensation and $N_\alpha$-deprotection reactions using **13** and **12** to furnish the linear dodecapeptide **28a**/**b**.

Next, the allyl group of the C-terminus of **28a**/**b** was chemoselectively removed by catalysis of $Pd(PPh_3)_4$ in the presence of excess morpholine,[46] generating the precursor **29a**/**b** for macrolactamization. Amide formation between the N- and C-termini of **29a**/**b** was attained by the action of PyBOP/2,4,6-collidine[47] under pseudo high-dilution conditions, realizing the on-resin cyclization of the 40-membered ring of **30a**/**b**. To complete the solid-phase total synthesis of **1** and **2**, conditions for the last global deprotection were individually optimized for **30a** and **30b**. Treatment of the fully protected deoxy analogue **30b** with 95% aqueous TFA at rt simultaneously realized cleavage from the resin and removal of the *t*-Bu, Boc, and Tr groups, releasing **2** into solution. After purification by reversed-phase HPLC, deoxy analogue **2** was obtained in 6.6% yield in 26 steps from **11**. In contrast to this successful result, application of the same TFA conditions to **30a** did not effect full detachment of the extra TBS group at D-OHAsn-2 to yield the parent natural product WAP-8294A2 (**1**). Higher temperature only resulted in low yielding generation of the desired **1**. Thus, we adopted a two-step approach to improve the deprotection efficacy. First, the reagent combination of TBAF and AcOH was used to remove the TBS group from **30a**, and then the resultant compound was subjected to 95% aqueous TFA at rt to deliver **1**, which was purified by reversed-phase HPLC. Consequently, the total yield of WAP-8294A2 (**1**) from **11** in 27 steps was 8.4%. The 91% and 90% average yields per step for assembly of **1** and **2**, respectively, demonstrated the high efficiency of the present full solid-phase synthetic strategy. All the spectral and physical data of **1**, including $^1$H NMR, $^{13}$C NMR, $[\alpha]_D$, and HRMS data, matched those of naturally occurring **1** (Tables S1 and S2).[11,12] In addition, the $^1$H and $^{13}$C NMR chemical shifts of **2** were in excellent agreement with those of **1**, and thus the deletion of the one hydroxy group from **1** was inconsequential to the three-dimensional core structure.

**Antimicrobial activity.** We next evaluated the antibacterial activities of the synthetically prepared **1** and **2** (Table 1). The MIC values were determined using the standard microdilution procedure against eight strains of Gram-positive bacteria, three strains of Gram-negative bacteria, and three strains of true fungi. The comparable MIC values of natural **1** (0.78 μg/mL) and synthetic **1** (2 μg/mL) on Methicillin-resistant *S. aureus* (MRSA) further confirmed their chemical equivalence. Compound **1** exhibited potent antimicrobial activity (2 μg/mL) against the six strains of Gram-positive bacteria (Methicillin-susceptible *S. aureus*, MRSA, S*taphylococcus simulans*, *Staphylococcus pseudintermedius*, *Bacillus subtilis*, and *Bacillus cereus*), whereas **1** was ineffective against the two strains of Gram-positive bacteria (*Streptococcus pyogenes* and *Streptococcus pneumoniae*), and all strains of Gram-negative bacteria (*Serratia marcescens*, *Escherichia coli*, and *Pseudomonas aeruginosa*) and true fungi

**Table 1. Antimicrobial activities of 1-3**

| strains | MIC (μg/mL)[a] | | |
|---|---|---|---|
| | **1** | **2** | **3** (ref 18) |
| **Gram-positive bacteria** | | | |
| Methicillin-susceptible *S. aureus* MSSA1 (clinical isolate) | 2 | 2 | 4 |
| Methicillin-resistant *S. aureus* MRSA4 (clinical isolate) | 2 | 2 | 4 |
| *Staphylococcus simulans* JCM2424 | 2 | 2 | 4 |
| *Staphylococcus pseudintermedius* JCM17571 | 2 | 2 | 4 |
| *Bacillus subtilis* JCM2499 | 2 | 2 | 4 |
| *Bacillus cereus* JCM20037 | 2 | 2 | 2 |
| *Streptococcus pyogenes* SS1-9 | 64 | 128 | >128 |
| *Streptococcus pneumoniae* (clinical isolate) | >128 | >128 | >128 |
| **Gram-negative bacteria** | | | |
| *Serratia marcescens* (clinical isolate) | >128 | >128 | >128 |
| *Escherichia coli* W3110 | >128 | >128 | >128 |
| *Pseudomonas aeruginosa* PAO1 | >128 | >128 | >128 |
| **True fungi** | | | |
| *Candida albicans* ATCC10231 | >128 | >128 | >128 |
| *Candida tropicalis* pK233 | >128 | >128 | >128 |
| *Cryptococcus neoformans* H99 | 64 | 64 | >128 |

[a]Antimicrobial activities against various bacteria and true fungi were determined by the microdilution method.

**Table 2. Antimicrobial activities against MK-deficient deletion mutants of *S. aureus***

| strains | MIC (μg/mL)[a] | | |
|---|---|---|---|
| | **1** | **2** | **3** (ref 18) |
| Wild-type (RN4220) | 4 | 4 | 4 |
| Δ*menA* | 128 | >128 | 64 |
| Δ*menB* | 128 | >128 | 64 |

[a]Antimicrobial activities against various bacteria were determined by the microdilution method.

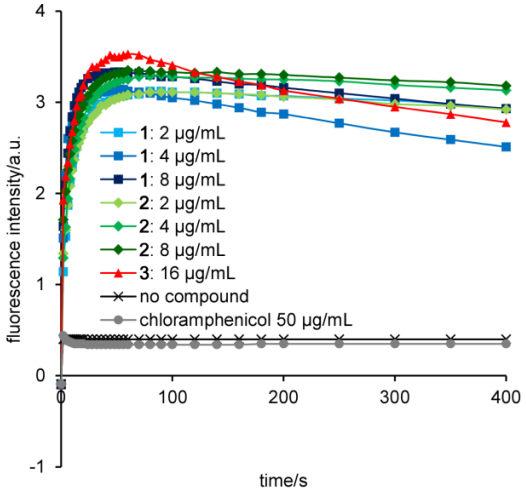


**Figure 3.** Change in the membrane potential of *S. aureus* after the addition of **1** and **2**. The change in membrane potential was monitored by the fluorescence of $DiSC_3(5)$ in the presence of 2, 4, or 8 μg/mL of **1** and **2**. Compound 3 (16 μg/mL) and chloramphenicol (50 μg/mL) were used as a positive control and a negative control, respectively. a.u.: arbitrary unit; $DiSC_3(5)$: 3,3'-dipropylthiadicarbocyanine iodide.

(*Candida albicans*, *Candida tropicalis*, and *Cryptococcus neoformans*). Intriguingly, deoxy analogue **2** had the same MIC values as **1** for all the tested strains except for *S. pyogenes*. These data uncovered the dispensability of the additional hydroxy group at D-OHAsn-2 for the antimicrobial activity.

The observed potency and spectrum of the activity of **1** and **2** were in accordance with those of lysocin E (**3**) (Table 1). Importantly, all of the three compounds displayed significantly low activities toward Gram-positive *S. pyogenes* and *S. pneumoniae* that lack MK within the membrane.[48] To further verify that the presence of MK affects the antimicrobial activities of **1** and **2**, we next used two MK-deficient mutants (Δ*menA* and Δ*menB*) of *S. aureus* RN4220 (Table 2).[19,49] MenB and MenA are involved in the formation of naphthoquinone and the attachment of an isoprenyl chain to naphthoquinone, respectively, in the MK biosynthesis pathway, and their deletion results in a complete loss of MK in *S. aureus*. Consistent with the substantial activity loss of the MK-targeting antibiotic **3** toward the deletion mutants, **1** and **2** had negligible activities against both the Δ*menA* and Δ*menB* mutants (128 and >128 μg/mL for **1** and **2**, respectively) compared to the wild-type (4 μg/mL). These findings indicated that the antimicrobial actions of **1** and **2** correlate with MK production.

**Evaluation of membrane potential.** The potent bactericidal function of lysocin E (**3**) originates from its membrane-disrupting activity.[18] For example, **3** caused a loss of membrane potential in *S. aureus* in the presence of 3,3'-dipropylthiadicarbocyanine iodide [$DiSC_3(5)$] as a fluorescent probe (Figure 3, red),[50] while the antibiotic chloramphenicol had no effect (gray). In this assay, both **1** and **2** were found to have the same function as **3**. Application of the solutions of **1** (blue) and **2** (green) in a concentration range similar to their MIC values (2-8 μg/mL) induced a rapid increase in the fluorescence of $DiSC_3(5)$, indicating loss of the membrane potential. These results strongly suggested that the antimicrobial activities of **1** and **2** are due to their effects to alter the functional integrity of the bacterial membrane.

**Menaquinone-dependent membrane lysis.** MK-dependent membrane-lysis of **1** and **2** was investigated using four types of liposomes, and compared with that of **3**. Large unilamellar vesicles (LUVs) comprising egg yolk phosphatidylcholine (PC)/egg yolk phosphatidylglycerol (PG) (50:50 ratio) and PC/PG/cardiolipin (CL) (50:40:10 ratio) were prepared to mimic the negatively-charged surface of bacterial membranes.[51] The PC/PG LUVs were doped with 1.25 mol% of MK-4 (**4**),[52,53] or with 1.25 mol% of UQ-10 (**5**) to access the selectivity of **1** and **2** toward MK over UQ. The total lipid concentration of each LUV solution was adjusted to 8 μM, and carboxyfluorescein (CF) was encapsulated as a fluorescent indicator in all four LUVs.[54] While fluorescence of the CF molecules within the LUVs is self-quenched due to the high concentration, an increase in fluorescence intensity can be observed when membrane disruption by peptides causes the CF to leak from LUVs, resulting in dilution of the CF molecules. Therefore, fluorescence was measured as an indicator of LUV membrane disruption. The fluorescence change (%) in the presence of each peptide was standardized according to the maximum intensity (100%) induced by adding Triton X-100. The membrane-disrupting activities of **1**-**3** toward the four types of LUVs were quantified as half-maximal response ($EC_{50}$) values by measuring fluorescence changes (%) of varied concentrations (0.0015 nM to 2970 nM) of **1**-**3** after reaching their plateaus (30 min).

Although all four LUVs could be ruptured dose-dependently by **1** and **2** (Figures 4a and b), the MK-4 (**4**)-containing LUVs were most responsive toward the addition of **1** and **2** (blue lines vs. red, black, and green lines). It therefore demonstrated a key role of MK in the membrane rupturing activities of **1** and **2**. The same MK-sensitive behavior was observed upon subjecting **3** to the four LUVs (Figure 4c). The $EC_{50}$ values of **1**, **2**, and **3** for the **4**-containing LUVs were calculated to be 14.2, 22.1, and 15.9 nM (Table 3), respectively. In contrast, 27 to 59 times higher concentrations were necessary to cause 50% leakage of the LUVs containing PC/PG ($EC_{50}$ = 503, 640, and 435 nM for **1**, **2**, and **3**, respectively) and PC/PG/CL ($EC_{50}$ = 833, 781, and 501 nM for **1**, **2**, and **3**, respectively). Furthermore, the $EC_{50}$ values of **1**, **2**, and **3** for UQ-10 (**5**)-containing-LUVs were 9.3-, 12-, and 3.6-fold larger than those for **4**-containing-LUVs ($EC_{50}$ = 132, 261, and 56.5 nM for **1**, **2**, and **3**, respectively).

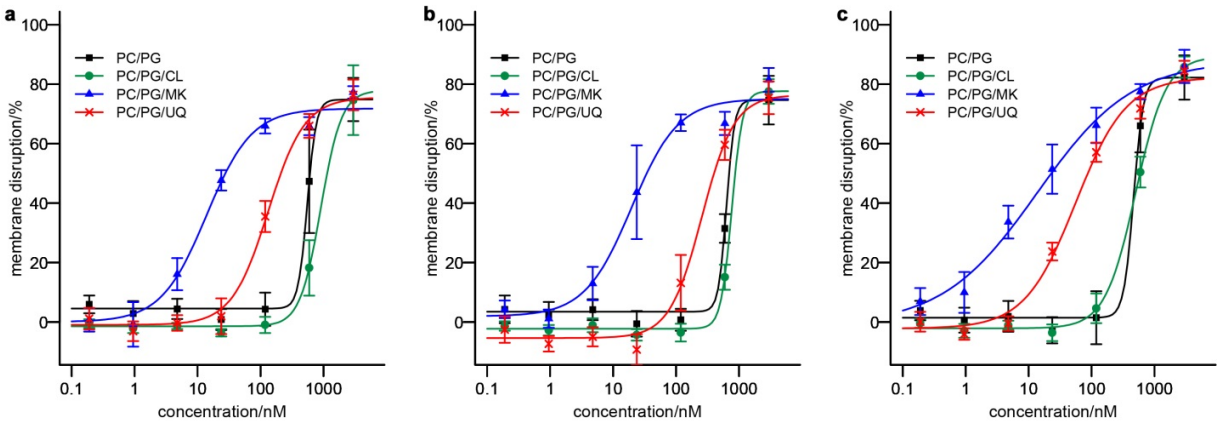


**Figure 4.** Comparison of dose-dependent membrane disrupting activities of **1** (a), **2** (b), and **3** (c) against the four LUVs [PC/PG = 50:50, PC/PG/CL = 50:40:10, PC/PG = 50:50 containing 1.25 mol% MK-4 (**4**) or UQ-10 (**5**)]. Egg yolk PC and egg yolk PG were used as PC and PG, respectively. The total lipid concentration of each LUV solution was adjusted to 8 μM. Mean values ± SD of three independent experiments are shown.

**Table 3. $EC_{50}$ values (nM) for the membrane-disrupting activities of 1, 2, and 3 against the four types of LUVs**

| compounds | $EC_{50}$ (nM) | | | |
|---|---|---|---|---|
| | PC/PG[a] | PC/PG /CL[b] | PC/PG /MK[c] | PC/PG /UQ[d] |
| **1** | 503 ± 165 | 833 ± 68 | 14.2 ± 3.1 | 132 ± 14 |
| **2** | 640 ± 39 | 781 ± 54 | 22.1 ± 12.9 | 261 ± 47 |
| **3** | 435 ± 83 | 501 ± 57 | 15.9 ± 7.3 | 56.5 ± 11.9 |

[a]PC/PG = 50:50, [b]PC/PG/CL = 50:40:10, [c]PC/PG = 50:50 containing 1.25 mol% MK-4 (**4**), [d]PC/PG = 50:50 containing 1.25 mol% UQ-10 (**5**). Egg yolk PC and egg yolk PG were used as PC and PG, respectively. The total lipid concentration of each LUV solution was adjusted to 8 μM. $EC_{50}$ values are displayed as mean ± SD of three independent experiments.

These liposome experiments validated the MK-dependency of the potent membrane lytic activities of **1** and **2**. The electrostatic interactions of positively-charged **1** and **2** with the negatively charged PG or CL did not lead to membrane disruption at micromolar concentrations of **1** and **2**, clarifying that PG and CL were not their specific targets. Addition of only 1.25 mol% of **4** to PC/PG enhanced the membrane lysis activities of **1** and **2** 29- to 35-fold, while addition of 1.25 mol% of the structurally related quinone **5** was much less effective for increasing the activities (2.5- to 3.8-fold). These membrane-disrupting and antimicrobial activities together strongly supported the MK-dependent mode of action by **1** and **2**. The selective molecular recognition of MK by **1** and **2** presumably leads to membrane damage and eventual bacterial death. Hence, we present WAP-8294A2 (**1**) and its deoxy analogue **2** as the first series of antibiotics that share the unique mechanism of lysocin E (**3**). It is worth noting that the MK/UQ-selectivity of **1** and **2** is higher than that of **3** (9.2 for **1**, 12 for **2**, and 3.6 for **3**), suggesting that **1** and **2** are superior to **3** as lead structures for developing optimal candidates of novel antibiotics.

## CONCLUSION

Here we report the first successful solid-phase total synthesis of the antibiotic peptide WAP-8294A2 (**1**) and its deoxy analogue (**2**), and their MK-dependent mode of action. After preparing preformed ester **14** and D-OHAsn-2 **15**, stepwise-elongation of the peptide chain from the side-chain anchored **11** gave rise to the dodecapeptide **28a**. Chemoselective deprotection of the C-terminus of **28a**, on-resin macrolactamization, and global deprotection delivered the complex 40-membered macrolactam **1**. Application of the same strategy except for the use of commercially available **12** in place of **15** realized the chemical construction of the more synthetically accessible **2**. The rapid and efficient access to **1** and **2** enabled detailed investigations of their biological functions. The equipotent antimicrobial activities of the parent natural product **1** and its deoxy analogue **2** indicate the biological insignificance of the hydroxy group on D-OHAsn-2. While **1** and **2** displayed the low MIC values toward the six strains of Gram-positive bacteria (2 μg/mL), the MK-deficient species (*S. pyogenes* and *S. pneumoniae*) and mutants (Δ*menA* and Δ*menB*) were highly resistant to **1** and **2**, suggesting a strong correlation between their antimicrobial activities and MK production. The membrane-disrupting effects of **1** and **2** were then validated by the loss of the membrane potential of *S. aureus*, and by the leakage of the encapsulated fluorescent molecules from the LUVs. Further, we determined the $EC_{50}$ values of **1** and **2** for lysis of four types of LUVs that differed in their membrane components. As a result, the activities of **1** and **2** was substantially enhanced by MK compared with the anionic lipids (PG and CL) or the structurally related quinone UQ. These data along with the similar assay results of lysocin E (**3**) supported that **1** and **2** selectively recognize MK present in the cytoplasmic membrane of Gram-positive bacteria, and kill the cells by disrupting their membranes. Thus, we present **1** and **2** as the first series of compounds that share the unique MK-targeting mode of action of **3**. As **1** and **2** exhibited higher selectivity toward MK over UQ than **3** in the LUV experiments, these compounds are potentially superior to **3** as the lead structures for drugs

with maximized antimicrobial activities and fewer undesirable side effects. Consequently, the present findings provide a new chemical basis for the development of MK-targeting next-generation antibiotics for the treatment of MRSA and various infectious diseases.

## EXPERIMENTAL SECTION

**General Methods.** All reactions sensitive to air and/or moisture were carried out under argon atmosphere in dry solvents, unless otherwise noted. THF, $CH_2Cl_2$, DMF, and $Et_2O$ were purified by a Glass Contour solvent dispensing system. All other reagents were used as supplied unless otherwise stated. Analytical thin-layer chromatography (TLC) was performed using 0.25 mm plates. Flash column chromatography was performed using 40–50 μm silica gel. Solid-phase peptide synthesis (SPPS) was performed on a microwave-assisted peptide synthesizer using a sealed reaction vessel, a reaction temperature of which was monitored by an internal temperature probe. Infrared (IR) spectra were recorded as a thin film on a KBr, NaCl, or $CaF_2$. $^1$H NMR spectra were recorded at 400 or 500 MHz. $^{13}$C NMR spectra were recorded at 100 or 125 MHz. Chemical shifts are denoted in $\delta$ (ppm) relative to residual solvent peaks as internal standard ($CDCl_3$, $^1$H $\delta$ 7.26, $^{13}$C $\delta$ 77.0; $CD_3OD$, $^1$H $\delta$ 3.31, $^{13}$C $\delta$ 49.0; DMSO-$d_6$, $^1$H $\delta$ 2.50, $^{13}$C $\delta$ 39.5). HRMS spectra were recorded on an electrospray ionization time-of-flight (ESI-TOF) mass spectrometer.

*β-keto ester **17***. To 5-methylhexanoic acid (**16**, 1.04 g, 7.98 mmol) was added thionyl chloride (754 μL, 10.4 mmol) at rt. The solution was heated to reflux, and stirred for 3 h. The reaction mixture was concentrated to give the crude acid chloride (810 mg), which was used in the next reaction without further purification.

To a solution of $LiN(TMS)_2$ (12.0 mmol) in THF (12.0 mL) was added AcOEt (642 μL, 6.54 mmol) over 5 min at −78 °C. The resultant solution was stirred at −78 °C for 30 min. A solution of the above crude acid chloride (810 mg) in THF (1.09 mL) was added to the solution over 7 min at −78 °C. The mixuture was stirred at −78 °C for 1 h, and then saturated aqueous $NH_4Cl$ (15 mL) was added. The resultant mixture was extracted with $Et_2O$ (30 mL ×1, 10 mL ×2). The combined organic layers were washed with brine (30 mL), dried over anhydrous $Na_2SO_4$, filtered, and concentrated. The residue was roughly purified by flash column chromatography on silica gel (20 g, pentane/$Et_2O$ 40/1 to 10/1) to give the crude **17** (807 mg), which was used in the next reaction without further purification.

*β-hydroxy ester **18***. A solution of benzeneruthenium(II) chloride dimer (49.9 mg, 99.9 μmol) and (*R*)-BINAP (124 mg, 0.200 mmol) in DMF (499 μL) was stirred at 100 °C for 10 min. The reaction mixture was concentrated to give the crude catalyst $RuCl_2$[(*R*)-BINAP](DMF)$_n$, which was used in the next reaction without further purification.

A solution of the above crude **17** (532 mg) and the above crude catalyst $RuCl_2$[(*R*)-BINAP](DMF)$_n$ in MeOH (1.00 mL) was transferred to an autoclave. The solution was stirred at rt under $H_2$ (10 bar) for 3 d. After venting $H_2$ at rt, the solution was concentrated. The residue was purified by flash column chromatography on silica gel (20 g, pentane/$Et_2O$ 25/1 to 5/1) to give **18** (451 mg, 35% over 3 steps): yellow oil; $[\alpha]_D^{27}$ = −19.4 (*c* = 1.37, $CHCl_3$); IR (film) $\nu$ 3446, 2954, 2931, 2870, 1733, 1458, 1372, 1174, 1036 cm$^{-1}$; $^1$H NMR (500 MHz, $CDCl_3$) $\delta$ 0.87 (6H, d, *J* = 6.3 Hz), 1.15-1.58 (10H, m), 2.40 (1H, dd, *J* = 16.6, 9.2 Hz), 2.50 (1H, dd, *J* = 16.6, 2.9 Hz), 2.94 (1H, d, *J* = 4.1 Hz), 3.90 (1H, m), 4.17 (2H, q, *J* = 7.5 Hz); $^{13}$C NMR (125 M Hz, $CDCl_3$) $\delta$ 14.2, 22.6 (2C), 23.2, 27.9, 36.7, 38.8, 41.3, 60.7, 68.0, 173.2; HRMS (ESI-TOF) calcd for $C_{11}H_{22}O_3Na$ [M+Na]$^+$ 225.1461, found 225.1469. The configuration of β-hydroxy group of **18** was determined to be *R* by the modified Mosher method.[55]

*Benzyl ester **19***. To a solution of **18** (327 mg, 1.62 mmol) in THF (9.34 mL) was added a solution of NaOH (747 mg, 18.7 mmol) in $H_2O$ (9.34 mL) at 0 °C. After being stirred at rt for 3.5 h, the solution was concentrated. The residue was dissolved in $H_2O$ (30 mL). The aqueous layer was washed with $Et_2O$ (20 mL). The aqueous layer was acidified (pH 1) with 4 M aqueous HCl (6 mL). The resultant solution was extracted with $Et_2O$ (20 mL ×3). The combined organic layers were washed with brine (40 mL), dried over anhydrous $Na_2SO_4$, filtered, and concentrated to give the crude carboxylic acid (268 mg), which was used in the next reaction without further purification.

To a solution of the above crude carboxylic acid (253 mg) in DMF (3.03 mL) were added $K_2CO_3$ (220 mg, 1.59 mmol) and benzyl bromide (189 μL, 1.59 mmol) at 0 °C. The reaction mixture was stirred at rt for 10 h, and then saturated aqueous $NH_4Cl$ (5 mL) was added. The resultant mixture was extracted with $Et_2O$ (10 mL ×3). The combined organic layers were washed with brine (15 mL), dried over anhydrous $Na_2SO_4$, filtered, and concentrated. The residue was purified by flash column chromatography on silica gel (20 g, hexane/AcOEt 10/1 to 5/1) to give **19** (346 mg, 90%): yellow oil; $[\alpha]_D^{23}$ = −14.4 (*c* = 1.15, $CHCl_3$); IR (film) $\nu$ 3446, 2953, 2931, 2869, 1733, 1457, 1384, 1261, 1166 cm$^{-1}$; $^1$H NMR (500 MHz, $CDCl_3$) $\delta$ 0.87 (6H, d, *J* = 6.3 Hz), 1.12-1.66 (7H, m), 2.47 (1H, dd, *J* = 16.6, 9.2 Hz), 2.56 (1H, dd, *J* = 16.6, 3.5 Hz), 4.03 (1H, m) 5.16 (2H, s), 7.31-7.40 (5H, m); $^{13}$C NMR (125 M Hz, $CDCl_3$) $\delta$ 22.5 (2C), 23.2, 27.9, 36.7, 38.8, 41.3, 66.5, 68.0, 128.3 (2C), 128.4, 128.6 (2C), 135.6, 172.9; HRMS (ESI-TOF) calcd for $C_{16}H_{24}O_3Na$ [M+Na]$^+$ 287.1618, found 287.1619. Enantiomeric excess of **19** was determined to be 97% ee of the *R*-enantiomer ($t_R$ = 20.3 min, Figure S1)[39] by normal phase chiral HPLC analysis (column: Chiralcel OD-H 4.6 ×250 mm, eluent A: hexane; eluent B: *i*-PrOH; 95% A/5% B, flow rate: 0.5 mL/min, detection: UV 210 nm).

*Ester **21***. To a solution of **19** (346 mg, 1.31 mmol) in $CH_2Cl_2$ (6.55 mL) were added *N*,*N*'-diisopropylcarbodiimide (DIC, 307 μL, 1.96 mmol), *N*,*N*-dimethyl-4-aminopyridine (DMAP, 48.0 mg, 0.552 mmol), and Fmoc-L-*N*-MeVal-OH (**20**, 509 mg, 1.44 mmol) at rt. The mixture was stirred at rt for 3 h. Then, **20** (231 mg, 0.655 mmol) and DIC (205 μL, 1.31 mmol) was added to the mixture. The solution was stirred at rt for 3 h, and

then saturated aqueous $NH_4Cl$ (6 mL) was added. The resultant mixture was extracted with $Et_2O$ (25 mL). The combined organic layers were washed with brine (20 mL), dried over anhydrous $Na_2SO_4$, filtered, and concentrated. The residue was purified by flash column chromatography on silica gel (30 g, hexane/AcOEt 20/1 to 10/1) to give **21** (716 mg, 91%): colorless oil; $[\alpha]_D^{20}$ = –46.5 (*c* = 0.714, $CHCl_3$); IR (film) $\nu$ 2957, 2870, 1739, 1703, 1452, 1307, 1197, 1169, 1149, 988 $cm^{-1}$; $^1H$ NMR (500 MHz, $CDCl_3$) Signals derived from rotamers A and B (1:1) were observed. $\delta$ 0.72 (1.5H, d, *J* = 6.9 Hz), 0.77-1.01 (10.5H, m), 1.07-1.35 (4.0H, m), 1.40-1.65 (3.0H, m), 2.04-2.21 (1.0H, m), 2.48-2.71 (2.0H, m), 2.82 (1.5H, s), 2.86 (1.5H, s), 4.06 (0.5H, d, *J* = 10.9 Hz), 4.21-4.27 (1.0H, m), 4.30-4.55 (2.5H, m), 5.01-5.12 (2.0H, m), 7.55-7.64 (2.0H, m), 7.73-7.79 (2.0H, m); $^{13}C$ NMR (125 MHz, $CDCl_3$) Signals derived from rotamers A and B were observed. $\delta$ 18.5 (A), 18.8 (B), 19.5 (A), 19.6 (B), 22.5 (2C of A and B), 22.9 (A and B), 27.0 (A), 27.4 (B), 27.8 (A and B), 34.1 (A and B), 38.5 (A and B), 39.1 (A and B), 47.3 (A and B), 64.0 (B), 64.3 (A), 66.4 (A or B), 66.6 (A or B), 67.5 (A), 67.6 (B), 67.6 (B), 71.1 (A and B), 119.9 (2C of A and B), 124.9 (2C of A or B), 125.0 (2C of A or B), 126.96 (A or B), 127.02 (2C of A or B), 127.1 (A or B), 127.7 (2C of A and B), 128.2 (2C of A and B), 128.3 (A and B), 128.5 (2C of A and B), 135.6 (A and B), 141.3 (2C of A or B), 141.4 (2C of A or B), 143.85 (A or B), 143.91 (A or B), 144.0 (A or B), 144.3 (A or B), 156.1 (A), 156.8 (B), 169.7 (A or B), 169.9 (A or B), 170.0 (A or B), 170.3 (A or B); HRMS (ESI-TOF) calcd for $C_{37}H_{45}NO_6Na$ $[M+Na]^+$ 622.3139, found 622.3147.

*Ester **14***. To a solution of **21** (1.02 g, 1.70 mmol) in AcOEt (34.0 mL) was added 5 wt% Pd/C (203 mg, 95.3 μmol) at rt. The flask equipped with a balloon was evacuated and recharged with $H_2$ (×3). After being stirred at rt for 3 h under $H_2$ atmosphere, the reaction mixture was filtered through a pad of Celite with AcOEt (30 mL). The filtrate was concentrated. The residue was purified by flash column chromatography on silica gel (60 g, hexane/AcOEt = 4/1 to 1/1) to give **14** (756 mg, 85%): white solid; m.p. 118-120 °C; $[\alpha]_D^{23}$ = –66.1 (*c* = 1.09, $CHCl_3$); IR (film) $\nu$ 2959, 2929, 2870, 1739, 1708, 1451, 1260, 1199, 1033 $cm^{-1}$; $^1H$ NMR (500 MHz, $CDCl_3$) Signals derived from rotamer A and B (1:1) were observed. $\delta$ 0.67 (1.5H, d, *J* = 6.9 Hz), 0.79-0.90 (9.0H, m), 0.99 (1.5H, d, *J* = 6.3 Hz), 1.08-1.38 (4.0H, m), 1.40-1.69 (3.0H, m), 2.08 (0.5H, m), 2.19 (0.5H, m), 2.41-2.67 (2.0H, m), 2.79 (1.5H, s), 2.87 (1.5H, s), 3.98 (0.5H, d, *J* = 11.5 Hz), 4.20-4.29 (1.0H, m), 4.37-4.56 (2.5H, m), 5.17-5.29 (1.0H, m), 7.28-7.34 (2.0H, m), 7.37-7.44 (2.0H, m), 7.57-7.68 (2.0H, m), 7.76 (2.0H, d, *J* = 7.5 Hz), 9.32 (1.0H, br); $^{13}C$ NMR (125 M Hz) Signals derived from rotamers A and B were observed. $\delta$ 18.3 (A), 18.7 (B), 19.4 (A), 19.6 (B), 22.4 (2C of A or B), 22.5 (2C of A or B), 22.9 (A and B), 26.6 (A), 27.3 (B), 27.8 (A and B), 29.6 (A), 30.0 (B), 34.05 (A or B), 34.14 (A or B), 38.40 (A or B), 38.44 (A or B), 38.77 (A or B), 38.79 (A or B), 47.2 (A and B), 64.0 (B), 64.2 (A), 67.5 (A), 67.7 (B), 70.8 (A or B), 70.9 (A or B), 119.85 (2C of A or B), 119.93 (2C of A or B), 124.8 (A or B), 124.9 (A or B), 124.98 (A or B), 125.02 (A or B), 126.9 (A or B), 127.01 (2C of A or B), 127.05 (A or B), 127.56 (A or B), 127.62 (A or B), 127.64 (2C of A or B), 141.26 (A or B), 141.29 (A or B), 141.34 (A or B), 141.4 (A or B), 143.8 (A or B), 143.9 (A or B), 144.0 (A or B), 144.3 (A or B), 156.3 (A), 156.9 (B), 169.4 (A), 170.2 (B), 174.6 (A), 175.4 (B); HRMS (ESI-TOF) calcd for $C_{30}H_{39}NO_6Na$ $[M+Na]^+$ 532.2670, found 532.2683.

*Benzyl ester **23***. A solution of monomethyl ester **22** (4.85 g, 18.4 mmol) in MeOH (136 mL) was bubbled with $NH_3$ at 0 °C for 4 h under sonication in a pressure tube. The tube was sealed and warmed to rt. After being stirred at rt for 2 d, the solution was concentrated to give the crude material, which was used in the next reaction without further purification.

To a solution of the above crude material in DMF (94.0 mL) were added $NaHCO_3$ (6.79 g, 80.8 mmol) and BnBr (6.92 mL, 58.3 mmol) at 0 °C. The mixture was stirred at rt for 21 h. Then, $NaHCO_3$ (1.58 g, 18.8 mmol) and BnBr (2.68 mL, 22.6 mmol) were added to the solution at 0 °C. The solution was stirred at rt for 19 h, and then $H_2O$ (250 mL) was added at 0 °C. The resultant mixture was extracted with AcOEt (150 mL ×3). The combined organic layers were washed with brine (150 mL), dried over anhydrous $Na_2SO_4$, filtered, and concentrated. The residue was purified by flash column chromatography on silica gel (200 g, $CH_2Cl_2$/MeOH 1/0 to 25/1) to give **23** (3.83 g, 60% over 2 steps): white foam; $[\alpha]_D^{24}$ = +24.6 (*c* = 0.765, $CHCl_3$); IR (film) $\nu$ 3354, 2979, 1694, 1682, 1504, 1368, 1254, 1162, 1106, 1060 $cm^{-1}$; $^1H$ NMR (500 MHz, $CD_3OD$) Signals derived from rotamers A and B (4:1) were observed. $\delta$ 1.34 (1.8H, s), 1.41 (7.2H, s), 4.53 (0.2H, s), 4.59 (0.8H, d, *J* = 2.3 Hz), 4.63 (0.2H, s), 4.70 (0.8H, d, *J* = 2.3 Hz), 5.17-5.26 (2.0H, m), 7.29-7.42 (5.0H, m); $^{13}C$ NMR (125 MHz, $CD_3OD$) $\delta$ 28.6 (3C), 58.2, 68.3, 72.8, 80.9, 129.1 (2C), 129.3, 129.5 (2C), 137.1, 158.1, 172.0, 176.6; HRMS (ESI-TOF) calcd for $C_{16}H_{22}N_2O_6Na$ $[M+Na]^+$ 361.1370, found 361.1373; $^1H$ NMR spectrum was identical with that of ***ent*-23**.[41,42]

*N-Trityl amide **24***. To a solid of **23** (3.83 g, 11.3 mmol) was added 4 M HCl in 1,4-dioxane (113 mL) at 0 °C. The resultant mixture was stirred at rt for 3.5 h, and concentrated to give the crude material, which was used in the next reaction without further purification.

To a solution of the above crude material in 1,4-dioxane/$H_2O$ (1/1, 113 mL) were added $NaHCO_3$ (5.71 g, 67.9 mmol) and FmocCl (2.93 g, 11.3 mmol) at 0 °C. After being stirred at rt for 2 h, the resultant suspension was diluted with $H_2O$ (100 mL) and AcOEt (800 mL). The organic layer was washed with 1 M aqueous HCl (400 mL ×2), saturated aqueous $NaHCO_3$ (400 mL) and brine (400 mL), dried over anhydrous $Na_2SO_4$, filtered, and concentrated. The residue was purified by flash column chromatography on silica gel (100 g, $CH_2Cl_2$/MeOH 1/0 to 25/2) to give Fmoc-protected amine, which was used in the next reaction without further purification.

To a solution of the above Fmoc-protected amine (2.07 g, 4.49 mmol) in AcOH (15.6 mL) were added TrOH (11.7 g, 44.9 mmol), $H_2SO_4$ (144 μL, 2.69 mmol), and $Ac_2O$ (1.06 mL, 11.2 mmol) at 50 °C. After being stirred at 50 °C for 2.5 h, the resultant suspension was diluted with AcOEt (200 mL) at rt. The resultant mixture was poured into

saturated aqueous $NaHCO_3$ (350 mL) at 0 °C with vigorous stirring. The organic layer was separated, and the aqueous layer was extracted with AcOEt (300 mL ×2). The combined organic layers were washed with brine (200 mL), dried over anhydrous $Na_2SO_4$, filtered, and concentrated. The residue was purified by flash column chromatography on silica gel (200 g, hexane/AcOEt 20/1 to 2/1) to give **24** (2.50 g, 35% over 3 steps): white foam; $[\alpha]_D^{24}$ = +12.5 (*c* = 0.303, $CHCl_3$); IR (film) $\nu$ 3370, 3061, 2921, 2851, 1726, 1666, 1513, 1494, 1448, 1207 $cm^{-1}$; $^1H$ NMR (400 MHz, $CDCl_3$) $\delta$ 4.17 (1H, t, *J* = 7.3 Hz), 4.26 (1H, dd, *J* = 10.5, 7.3 Hz), 4.38 (1H, dd, *J* = 10.5, 7.3 Hz), 4.57 (2H, m), 4.84 (1H, d, *J* = 9.6 Hz), 5.19 (2H, s), 5.96 (1H, d, *J* = 9.2 Hz), 7.14-7.30 (22H, m), 7.39 (2H, m), 7.54 (2H, m), 7.75 (2H, m), 7.94 (1H, s); $^{13}C$ NMR (125 MHz, $CDCl_3$) $\delta$ 46.9, 56.4, 67.78, 67.82, 70.5, 72.9, 119.9 (2C), 125.2 (2C), 127.1 (2C), 127.2 (3C), 127.7 (2C), 128.0 (6C), 128.1 (2C), 128.5, 128.55 (6C), 128.60 (2C), 134.7, 141.2 (2C), 143.6 (2C), 144.1 (3C), 157.0, 170.3, 170.6; HRMS (ESI-TOF) calcd for $C_{45}H_{38}N_2O_6Na$ $[M+Na]^+$ 725.2622, found 725.2611; $^1H$ NMR spectrum was identical with that of ***ent*-24**.[41,42]

*Silyl ether* ***25***. To a solution of **24** (2.45 g, 3.49 mmol) and 2,6-lutidine (1.62 mL, 14.0 mmol) in $CH_2Cl_2$ (34.9 mL) was added TBSOTf (1.60 mL, 6.98 mmol) at 0 °C. After being stirred at 0 °C for 0.5 h, the reaction mixture was diluted with $Et_2O$ (150 mL), washed with 0.1 M aqueous HCl (150 mL ×3), saturated aqueous $NaHCO_3$ (150 mL) and brine (150 mL), dried over anhydrous $Na_2SO_4$, filtered, and concentrated. The residue was purified by flash column chromatography on silica gel (50 g, hexane/AcOEt 10/1 to 3/1) to give **25** (2.71 g, 95%): white foam; $[\alpha]_D^{26}$ = +13.1 (*c* = 2.53, $CHCl_3$); IR (film) $\nu$ 3410, 2927, 2856, 1730, 1693, 1494, 1448, 1254, 1197, 1104 $cm^{-1}$; $^1H$ NMR (500 MHz, $CDCl_3$) Signals derived from rotamers A and B (4:1) were observed. $\delta$ –0.02 (2.4H, s), 0.00 (1.2H, s), 0.05 (2.4H, s), 0.82 (7.2H, s), 0.84 (1.8H, s), 4.10 (0.2H, m), 4.17-4.26 (1.6H, m), 4.31 (0.2H, m), 4.47 (0.8H, dd, *J* = 9.7, 6.3 Hz), 4.54 (0.8H, d, *J* = 2.3 Hz), 4.70 (0.2H, s), 4.88 (0.8H, dd, *J* = 10.0, 2.6 Hz), 4.97 (0.2H, d, *J* = 10.3 Hz), 5.13 (1.0 H, d, *J* = 12.6 Hz), 5.18 (1.0 H, d, *J* = 12.6 Hz), 5.42 (0.2H, d, *J* = 10.9 Hz), 5.95 (0.8H, d, *J* = 10.3 Hz), 7.11-7.60 (28.0H, m), 7.71-7.84 (3.0H, m); $^{13}C$ NMR (125 MHz, $CDCl_3$) Signals derived from rotamer A and B were observed. $\delta$ –5.4 (B), –5.3 (A), –5.1 (A), –4.8 (B), 17.7 (A and B), 25.5 (3C of A and B), 47.0 (A and B), 57.3 (A), 57.9 (B), 67.5 (A), 67.6 (A), 67.7 (B), 67.9 (B), 70.5 (A and B), 73.4 (A) 73.6 (B), 119.9 (2C of A and B), 125.1 (A and B), 125.3 (A and B), 127.0 (2C of A and B), 127.2 (3C of A and B), 127.6 (2C of A and B), 128.0 (8C of A and B), 128.4 (A and B), 128.5 (2C of A and B), 128.6 (6C of A and B), 134.6 (B), 134.7 (A), 141.1 (A and B), 141.2 (A and B), 143.6 (A and B), 143.9 (A and B), 144.1 (3C of A and B), 155.4 (B), 155.9 (A), 168.5 (B), 169.0 (A), 169.9 (A), 170.1 (B); HRMS (ESI-TOF) calcd for $C_{51}H_{52}N_2O_6SiNa$ $[M+Na]^+$ 839.3487, found 839.3511.

*Carboxylic acid* ***15***. To a solution of **25** (2.64 g, 3.23 mmol) in AcOEt/EtOH (1/1, 60.0 mL) was added a suspension of 10 wt% Pd/C (227 mg, 0.213 mmol) in AcOEt/EtOH (1/1, 4.60 mL) at rt. The flask equipped with a balloon was evacuated and recharged with $H_2$ (×3). After being stirred at rt for 40 min under $H_2$ atmosphere, the reaction mixture was filtered through a pad of Celite with AcOEt (30 mL) and EtOH (30 mL). The filtrate was concentrated. The residue was purified by flash column chromatography on silica gel (50 g, $CH_2Cl_2$/MeOH = 1/0 to 10/1) to give **15** (2.14 g, 91%): white foam; $[\alpha]_D^{25}$ = +15.8 (*c* = 0.628, $CHCl_3$); IR (film) $\nu$ 3405, 2928, 1722, 1692, 1493, 1448, 1256, 1211, 1105, 1056 $cm^{-1}$; $^1H$ NMR (400 MHz, DMSO-$d_6$) Signals derived from rotamer A and B (7:3) were observed. $\delta$ –0.08-0.12 (6.0H, m), 0.79-0.95 (9.0H, m), 4.00-4.71 (5.0H, m), 6.96-7.94 (24.0H, m), 8.20 (0.7H, s), 8.32 (0.3H, s); $^{13}C$ NMR (100 M Hz, DMSO-$d_6$) $\delta$ –5.3, –4.9, 17.8, 25.7 (3C), 46.7, 57.6, 66.3, 69.6, 73.9, 120.1 (2C), 125.4, 125.7, 126.8 (3C), 127.1, 127.2, 127.6 (6C), 127.7 (2C), 128.5 (6C), 140.7, 140.8, 143.7 (2C), 144.3 (3C), 156.6, 168.8, 171.5; HRMS (ESI-TOF) calcd for $C_{44}H_{46}N_2O_6SiNa$ $[M+Na]^+$ 749.3017, found 749.3009.

*Determination of loading rate of* ***11***. Resin **11** was treated with piperidine/NMP (1/4, 1.00 mL) at rt for 15 min. The supernatant was collected. The resin was again treated with piperidine/NMP (1/4, 1.00 mL) at rt for 15 min. The supernatant was collected. The resin was washed with NMP (2 mL ×4), and then the supernatant was collected. UV absorption at 301 nm of the combined supernatants was measured. The background absorbance was canceled by subtracting the control absorbance obtained from a solution of piperidine/NMP (1/24). The loading rate (*x* mmol/g) was determined by the following equation, where *a* is the weight of **11** (mg), and *b* is absorbance at 301 nm.

$$x = (10000 \times b) / (7800 \times a)$$

*Procedures for solid-phase peptide synthesis.* Peptides **1** and **2** were prepared on a peptide synthesizer. Standard operation was shown as follows:

Step 1: The solid supported N-Fmoc peptide was deprotected with piperidine/NMP (1/4) at rt for 10 min.

Step 2: The reaction vessel (LibraTube) containing the resin was washed with NMP (5 mL ×6 for synthesis of **1**, 2 mL ×6 for synthesis of **2**).

Step 3: A Fmoc-amino acid (4.0 eq) was activated by a solution of *O*-(7-azabenzotriazole-1-yl)-*N*,*N*,*N*',*N*'-tetramethyluronium hexafluorophosphate (HATU)/1-hydroxy-7-azabenzotriazole (HOAt) (4.0 eq, 0.45 M) in NMP. To the solution of activated Fmoc-amino acid was added a solution of *i*-$Pr_2NEt$ (8.0 eq, 2.0 M) in NMP. The resultant mixture was transferred to the reaction vessel.

Step 4: The activated Fmoc-amino acid was coupled with the peptide on the resin (40 °C, 200 W; 20 min) and the reaction vessel containing the resin was washed with NMP (5 mL ×6 for synthesis of **1**, 2 mL ×6 for synthesis of **2**).

Steps 1–4 were repeated and amino acids were condensed on the solid support.

*WAP-8294A2 (lotilibcin,* ***1****).* To a solution of Fmoc-L-Glu-OAllyl (1.05 g, 2.57 mmol) in $CH_2Cl_2$/NMP (30/1, 38.9 mL) was added *N*-*N*'-diisopropylcarbodiimide (DIC, 413 μL, 2.67 mmol) at rt. After being stirred at rt for 20 min,

the solution was concentrated to give the crude acid anhydride, which was used in the next reaction without further purification.

Wang-ChemMatrix resin (1.01 g, 0.513 mmol) in 20 mL LibraTube was washed with $CH_2Cl_2$ (5 mL ×3) and NMP (5 mL ×5). To the resin were added a solution of the above crude acid anhydride in NMP (6.88 mL) and a solution of DMAP (6.27 mg, 51.3 μmol) in NMP (0.627 mL). After being stirred at rt for 1 h, the reaction mixture was filtered, and washed with NMP (5 mL ×5) and $CH_2Cl_2$ (5 mL ×5). To the resin was added $Ac_2O/CH_2Cl_2$ (1/3, 6 mL). After being stirred at rt for 20 min, the reaction mixture was filtered, washed with $CH_2Cl_2$ (5 mL ×5), MeOH (5 mL ×5), and $Et_2O$ (5 mL ×5), and dried under vacuum to give **11** (1.19 g, 72%). The loading rate was determined to be 0.265 mmol/g by the above method.

The above resin **11** (391 mg, 0.104 mmol) in 20 mL LibraTube was washed with $CH_2Cl_2$ (5 mL ×3) and NMP (5 mL ×6). The resin was subjected to 8 cycles (**10**, **9**, **8**, **7**, **6**, **15**, **6**, and **14**) of the microwave-assisted SPPS protocol to give peptide **26a**.

The resin-bound peptide **26a** was subjected to steps 3 and 4 of the microwave-assisted SPPS protocol using **10** (188 mg, 0.414 mmol), which was performed by the double coupling method (90 min ×2, steps 3 and 4 were repeated before step 1). After the 2 cycles of condensation of **10**, deprotection of N-Fmoc group was performed for 1 min. The reaction mixture was washed with NMP (5 mL ×6) to give peptide **27a**.

The resin-bound peptide **27a** was subjected to 2 cycles (**13** and **12**) of the microwave-assisted SPPS protocol. After the final Fmoc deprotection, the reaction mixture was washed with $CH_2Cl_2$ (5 mL ×6) to give peptide **28a**.

To the resin-bound peptide **28a** in 20 mL LibraTube was added a solution of $Pd(PPh_3)_4$ (31.1 mg, 26.9 μmol) and morpholine (179 μL, 2.07 mmol) in $CH_2Cl_2$ (3.45 mL). After being stirred at rt for 0.5 h, the reaction mixture was washed with $CH_2Cl_2$ (5 mL ×6), NMP (5 mL ×6), and NMP/$CH_2Cl_2$ (1/9, 5 mL ×6) to give peptide **29a**.

To the resin-bound peptide **29a** in 20 mL LibraTube was added a solution of PyBOP (226 mg, 0.435 mmol) and 2,4,6-collidine (112 μL, 0.850 mmol) in NMP/$CH_2Cl_2$ (1/9, 2.59 mL). After being stirred at rt for 12 h, the reaction mixture was washed with $CH_2Cl_2$ (5 mL ×6), NMP (5 mL ×6), MeOH (5 mL ×6), and $Et_2O$ (5 mL ×6), and dried under vacuum to give peptide **30a**.

The resin-bound peptide **30a** was washed with THF (5 mL ×6). To the resin-bound peptide was added a solution of TBAF (81.2 mg, 0.311 mmol) and AcOH (17.8 μL, 0.311 mmol) in THF (3.45 mL). After being stirred at rt for 0.5 h, the reaction mixture was washed with THF (5 mL ×6) and $Et_2O$ (5 mL ×6), and dried under vacuum.

To the resin-bound peptide was added 95% aqueous TFA (8.0 mL). After being stirred for 2 h, the reaction mixture was filtered, and washed with 95% aqueous TFA (5.0 mL ×6). The filtrate was concentrated to give the crude **1**. The crude **1** was dissolved in MeOH, filtered, and concentrated. The residue was purified by 1st reversed-phase HPLC (column: Inertsil ODS-3 20 ×250 mm, eluent A: MeOH + 0.05% TFA, eluent B: $H_2O$ + 0.05% TFA, linear gradient A/B = 72/28 to 82/18 over 40 min, flow rate: 4.0 mL/min, detection: UV 280 nm), 2nd reversed-phase HPLC (column: Inertsil ODS-3 20 ×250 mm, eluent A: MeCN + 0.05% TFA, eluent B: $H_2O$ + 0.05% TFA, A/B = 43/57, flow rate: 4.0 mL/min, detection: UV 280 nm), and 3rd reversed-phase HPLC (column: Inertsil C8-3 10 ×250 mm, eluent A: MeOH + 0.05% TFA, eluent B: $H_2O$ + 0.05% TFA, linear gradient A/B = 60/40 to 80/20 over 50 min, flow rate: 3.0 mL/min, detection: UV 280 nm) to give **1** ($t_R$ = 35.7 min, 14.7 mg, 8.4 % over 27 steps): white solid; $[\alpha]_D^{26}$ = +29.8 (*c* = 0.303, MeOH); IR (film) $\nu$ 3277, 2956, 1730, 1672, 1632, 1540, 1436, 1203, 1137 $cm^{-1}$; $^1H$ NMR (500 MHz, DMSO-$d_6$) 3-OH-7-Me-octanoic acid $\delta$ 2.33 ($H^2$), 2.56 ($H^{2'}$), 4.95 ($H^3$), 1.52 ($H^4$), 1.24 ($H^5$), 1.13 ($H^6$), 1.48 ($H^7$), 0.84 ($H^8$, $H^{8'}$); L-Ser-1 $\delta$ 4.79 ($H^\alpha$), 3.49 ($H^\beta$), 3.60 ($H^{\beta'}$), 7.93 (N*H*); D-OHAsn-2 $\delta$ 4.95 ($H^\alpha$), 4.28 ($H^\beta$), 7.34 ($NH^\gamma$), 7.37 ($NH^{\gamma'}$), 8.04 (N*H*), 5.72 ($OH^\beta$); L-Ser-3 $\delta$ 4.80 ($H^\alpha$), 3.64 ($H^\beta$), 8.23 (N*H*); Gly-4 $\delta$ 3.89 ($H^\alpha$), 8.15 (N*H*); N-Me-D-Phe-5 $\delta$ 4.48 ($H^\alpha$), 2.95 ($H^\beta$), 3.27 ($H^{\beta'}$), 7.17 ($H^2$, $H^6$), 7.28 ($H^3$, $H^5$), 7.19 ($H^4$), 2.61 ($NCH_3$); L-Leu-6 $\delta$ 4.30 ($H^\alpha$), 1.39 ($H^\beta$), 1.58 ($H^{\beta'}$), 1.40 ($H^\gamma$), 0.71 ($H^\delta$), 0.73 ($H^\gamma$), 7.94 (N*H*); D-Orn-7 $\delta$ 4.63 ($H^\alpha$), 1.66 ($H^\beta$), 1.71 ($H^{\beta'}$), 1.54 ($H^\gamma$), 2.86 ($H^\delta$), 7.81 ($NH_2$), 7.49 (N*H*); L-Glu-8 $\delta$ 4.62 ($H^\alpha$), 1.73 ($H^\beta$), 1.86 ($H^{\beta'}$), 2.20 ($H^\gamma$), 8.46 (N*H*), 12.09 ($OH^\delta$); D-Asn-9 $\delta$ 4.78 ($H^\alpha$), 2.45 ($H^\beta$), 2.62 ($H^{\beta'}$), 6.92 ($NH^\gamma$), 7.33 ($NH^{\gamma'}$), 8.16 (N*H*); D-Trp-10 $\delta$ 4.72 ($H^\alpha$), 2.81 ($H^\beta$), 3.13 ($H^{\beta'}$), 7.14 ($H^2$), 7.46 ($H^4$), 6.91 ($H^5$), 6.97 ($H^6$), 7.31 ($H^7$), 10.30 ($NH^1$), 8.65 (N*H*); D-Orn-11 $\delta$ 4.60 ($H^\alpha$), 1.58 ($H^\beta$), 1.70 ($H^{\beta'}$), 1.45 ($H^\gamma$), 2.82 ($H^\delta$), 7.81 ($NH_2$), 7.98 (N*H*); N-Me-L-Val-12 $\delta$ 4.62 ($H^\alpha$), 2.08 ($H^\beta$), 0.74 ($H^\gamma$), 0.88 ($H^{\gamma'}$), 2.57 ($NCH_3$); $^{13}C$ NMR (125 MHz, DMSO-$d_6$) $\delta$ 18.0, 19.1, 20.8, 22.0, 22.2, 22.9, 23.0, 23.2, 24.1, 25.7, 27.2, 27.4, 28.1, 28.4, 29.4, 29.8, 30.2, 33.1, 34.0, 34.7, 38.1, 38.1, 38.4, 38.5, 38.6, 39.3 (overlapped with $CHD_2S(O)CD_3$, determined from $^1H$-$^{13}C$ HMQC correlation), 42.0, 48.3, 49.2, 50.8, 51.2, 51.3, 52.7, 54.1, 54.8, 54.9, 61.0, 62.0, 62.7, 62.8, 71.0, 71.2, 109.4, 111.3, 118.0, 118.1, 120.6, 123.3, 126.2, 127.2, 128.2, 129.0, 135.9, 138.2, 169.0, 169.1, 169.2, 169.3, 169.3, 169.6, 169.8, 169.9, 170.4, 170.5, 170.7, 171.0, 171.5, 171.8, 173.5, 173.9; HRMS (ESI-TOF) calcd for $C_{73}H_{112}N_{17}O_{21}^+$ $[M+H]^+$ 1562.8213, found 1562.8232.

*Peptide* **2**. To a solution of Fmoc-L-Glu-OAllyl (261 mg, 0.637 mmol) in $CH_2Cl_2$/NMP (30/1, 9.64 mL) was added DIC (98.7 μL, 0.637 mmol) at rt. After being stirred at rt for 20 min, the solution was concentrated to give the crude acid anhydride, which was used in the next reaction without further purification.

Wang-ChemMatrix resin (209 mg, 0.127 mmol) in 5 mL LibraTube was washed with $CH_2Cl_2$ (2 mL ×3) and NMP (2 mL ×3). To the resin were added a solution of the above crude acid anhydride in NMP (1.72 mL) and a solution of DMAP (1.56 mg, 12.7 μmol) in NMP (0.156 mL). After being stirred at rt for 1 h, the reaction mixture was filtered, and washed with NMP (2 mL ×3) and $CH_2Cl_2$ (2 mL ×3). To the resin was added $Ac_2O/CH_2Cl_2$ (1/3, 2 mL). After being stirred at rt for 20 min, the reaction mixture was

filtered, washed with $CH_2Cl_2$ (2 mL ×3), MeOH (2 mL ×3) and $Et_2O$ (2 mL ×6), and dried under vacuum to give **11** (254 mg, 73%). The loading rate was determined to be 0.366 mmol/g by the above method.

The above resin **11** (108 mg, 39.6 μmol) in 5 mL LibraTube was washed with $CH_2Cl_2$ (2 mL ×3) and NMP (2 mL ×3). The resin was was subjected to 5 cycles (**10**, **9**, **8**, **7**, and **6**) of the microwave-assisted SPPS protocol and washed with NMP (2 mL ×6), $CH_2Cl_2$ (2 mL ×6), MeOH (2 mL ×6), and $Et_2O$ (2 mL ×6), and dried under vacuum to give the resin-bound peptide (217 mg).

The resin-bound peptide (131 mg, 23.9 μmol) in 5 mL LibraTube was washed with $CH_2Cl_2$ (2 mL ×3) and NMP (2 mL ×3). The resin-bound peptide was subjected to 3 cycles (**12**, **6**, and **14**) of the microwave-assisted SPPS protocol to give peptide **26b**.

The resin-bound peptide **26b** was subjected to steps 3 and 4 of the microwave-assisted SPPS protocol using **10** (43.5 mg, 95.6 μmol), which was performed by the double coupling method (90 min ×2, steps 3 and 4 were repeated before step 1). After the 2 cycles of condensation of **10**, deprotection of N-Fmoc group was performed for 1 min. The reaction mixture was washed with NMP (2 mL ×6) to give peptide **27b**.

The resin-bound peptide **27b** was subjected to 2 cycles (**13** and **12**) of the microwave-assisted SPPS protocol. After the final Fmoc deprotection, the reaction mixture was washed with $CH_2Cl_2$ (2 mL ×6) to give peptide **28b**.

To the resin-bound peptide **28b** in 5 mL LibraTube was added a solution of $Pd(PPh_3)_4$ (7.18 mg, 6.22 μmol) and morpholine (41.2 μL, 0.478 mmol) in $CH_2Cl_2$ (0.797 mL). After being stirred at rt for 30 min, the reaction mixture was washed with $CH_2Cl_2$ (2 mL ×6), NMP (2 mL ×6), and NMP/$CH_2Cl_2$ (1/9, 2 mL ×6) to give peptide **29b**.

To the resin-bound peptide **29b** in 5 mL LibraTube was added a solution of PyBOP (52.0 mg, 0.100 mmol) and 2,4,6-collidine (25.9 μL, 0.196 mmol) in NMP/$CH_2Cl_2$ (1/9, 0.598 mL). After being stirred at rt for 18 h, the reaction mixture was washed with $CH_2Cl_2$ (2 mL ×6), NMP (2 mL ×6), $CH_2Cl_2$ (2 mL ×6), MeOH (2 mL ×6), and $Et_2O$ (2 mL ×6), and dried under vacuum to give peptide **30b**.

To the resin-bound peptide **30b** was added 95% aqueous TFA (3.0 mL). After being stirred for 2 h, the reaction mixture was filtered, and washed with 95% aqueous TFA (2.0 mL ×6). The filtrate was concentrated to give the crude **2**. The crude **2** was dissolved in MeOH, filtered, and concentrated. The residue was purified by reversed-phase HPLC (column: Inertsil ODS-4 10 ×250 mm, eluent A: MeOH + 0.05% TFA, eluent B: $H_2O$ + 0.05% TFA, linear gradient A/B = 70/30 to 85/15 over 40 min, flow rate: 3.0 mL/min, detection: UV 280 nm) to give **2** ($t_R$ = 25.2 min, 2.62 mg, 6.6 % over 26 steps): white solid; $[\alpha]_D^{25}$ = +36.7 (*c* = 0.169, MeOH); IR (film) $\nu$ 3277, 2957, 2359, 1722, 1631, 1547, 1440, 1204, 1138 $cm^{-1}$; $^1H$ NMR (500 MHz, DMSO-$d_6$) 3-OH-7-Me-octanoic acid $\delta$ 2.32 ($H^2$), 2.55 ($H^{2'}$), 4.95 ($H^3$), 1.49 ($H^4$), 1.24 ($H^5$), 1.13 ($H^6$), 1.48 ($H^7$), 0.82 ($H^8$, $H^{8'}$); L-Ser-1 $\delta$ 4.66 ($H^\alpha$), 3.50 ($H^\beta$), 3.57 ($H^{\beta'}$), 7.92 (N*H*); D-Asn-2 $\delta$ 4.87 ($H^\alpha$), 2.51 ($H^\beta$), 2.58 ($H^{\beta'}$) 6.96 (N$H^\gamma$), 7.39 (N$H^{\gamma'}$), 8.23 (N*H*); L-Ser-3 $\delta$ 4.80 ($H^\alpha$), 3.62 ($H^\beta$), 8.34 (N*H*); Gly-4 $\delta$ 3.88 ($H^\alpha$), 8.16 (N*H*); N-Me-D-Phe-5 $\delta$ 4.43 ($H^\alpha$), 2.96 ($H^\beta$), 3.27 ($H^{\beta'}$), 7.17 ($H^2$, $H^6$), 7.27 ($H^3$, $H^5$), 7.19 ($H^4$), 2.59 (N$CH_3$); L-Leu-6 $\delta$ 4.28 ($H^\alpha$), 1.38 ($H^\beta$), 1.51 ($H^{\beta'}$), 1.40 ($H^\gamma$), 0.69 ($H^\delta$), 0.72 ($H^\gamma$), 7.89 (N*H*); D-Orn-7 $\delta$ 4.62 ($H^\alpha$), 1.64 ($H^\beta$), 1.70 ($H^{\beta'}$), 1.56 ($H^\gamma$), 2.84 ($H^\delta$), 7.81 (N$H_2$), 7.53 (N*H*); L-Glu-8 $\delta$ 4.67 ($H^\alpha$), 1.74 ($H^\beta$), 1.86 ($H^{\beta'}$), 2.19 ($H^\gamma$), 8.49 (N*H*), 12.10 (O$H^\delta$); D-Asn-9 $\delta$ 4.76 ($H^\alpha$), 2.46 ($H^\beta$), 2.57 ($H^{\beta'}$), 6.92 (N$H^\gamma$), 7.39 (N$H^{\gamma'}$), 8.29 (N*H*); D-Trp-10 $\delta$ 4.73 ($H^\alpha$), 2.82 ($H^\beta$), 3.14 ($H^{\beta'}$), 7.12 ($H^2$), 7.47 ($H^4$), 6.91 ($H^5$), 6.97 ($H^6$), 7.32 ($H^7$), 10.33 (N$H^1$), 8.62 (N*H*); D-Orn-11 $\delta$ 4.60 ($H^\alpha$), 1.55 ($H^\beta$), 1.71 ($H^{\beta'}$), 1.45 ($H^\gamma$), 2.80 ($H^\delta$), 7.81 (N$H_2$), 7.99 (N*H*); N-Me-L-Val-12 $\delta$ 4.63 ($H^\alpha$), 2.08 ($H^\beta$), 0.72 ($H^\gamma$), 0.87 ($H^{\gamma'}$), 2.56 (N$CH_3$); $^{13}C$ NMR (125 MHz, DMSO-$d_6$) $\delta$ 18.0, 19.1, 20.8, 22.0, 22.2, 22.9, 23.0, 23.2, 24.1, 25.7, 27.2, 27.4, 28.1, 28.3, 29.4, 29.8, 30.1, 33.1, 33.9, 34.9, 38.1, 38.1, 38.4, 38.4, 38.4, 38.6, 39.3 (overlapped with C*H*$D_2$S(O)C$D_3$, determined from $^1H$-$^{13}C$ HMQC correlation), 42.0, 48.4, 49.3, 49.4, 50.8, 51.2, 51.3, 52.7, 54.1, 54.8, 61.0, 62.1, 62.4, 63.0, 71.0, 109.4, 111.3, 118.0, 118.0, 120.6, 123.2, 126.2, 127.2, 128.2, 129.0, 135.9, 138.3, 169.1, 169.1, 169.3, 169.4, 169.5, 169.7, 170.0, 170.4, 170.4, 170.6, 170.7, 171.0, 171.5, 171.7, 171.9, 173.8; HRMS (ESI-TOF) calcd for $C_{73}H_{112}N_{17}O_{20}^+$ $[M+H]^+$ 1546.8264, found 1546.8236.

*Antimicrobial Activity Assay.* The MIC assay was performed according to the Clinical and Laboratory Standards Institute protocols. The antimicrobial and antifungal activities of each compound were measured using the microdilution method.[56,57]

*Evaluation of Membrane Potential.* Membrane potential was measured using the fluorescence assay.[58] *S. aureus* MSSA1 strain was grown to the mid-log phase in cation adjusted Mueller-Hinton broth medium. Cells were washed with 5 mM HEPES buffer, pH 7.0, 50 mM glucose, 5 mM EDTA, and resuspended in the same buffer to obtain an $A_{600}$ of 0.05. $DiSC_3(5)$ (3,3′-dipropylthiadicarbocyanine iodide) dye was added to a final concentration of 250 nM and cells were incubated in a water bath maintained at 37˚C for 15 min. The fluorescence emission was measured at 670 nm with the excitation at 622 nm using a spectrofluorometer equipped with a chamber heated at 37 °C. Data were collected for 400 s after addition of each compound.

*Preparation of CF-encapsulated LUVs consisting of PC/PG.* Carboxyfluorescein (CF)-encapsulated large unilamellar vesicles (LUVs) were prepared according to the thin-film hydration method, followed by extrusion through polycarbonate filters mounted in the extrusion apparatus. A solution of egg yolk phosphatidylcholine (EYPC, 9.60 mg, 12.5 μmol) and egg yolk phosphatidylglycerol (EYPG, 9.78 mg, 12.5 μmol) in $CHCl_3$ (0.505 mL) was concentrated, and dried under vacuum to form a lipid thin film. The thin film was hydrated and suspended in CF-containing buffer solution (0.500 mL, 5 mM HEPES, 20 mM CF, pH 7.5) by vortexing and sonication. After five-times freeze-thaw cycles, the lipid suspension was extruded 19 times through a polycarbonate filter with

0.40 μm of pore size in the diameter. The external CF-containing buffer was replaced with a CF-free buffer solution, (20 mM HEPES, 1 mM EDTA, pH 7.5) through size exclusion chromatography using disposable PD-10 column. Concentration of EYPC was determined by using Phospholipid C-Test Wako. The final concentration of EYPC was adjusted to 4.0 μM with the CF-free buffer solution, and used for membrane disruption assay.

*Preparation of CF-encapsulated LUVs consisting of PC/PG/CL.* To a solution of EYPC (4.80 mg, 6.25 μmol) and EYPG (3.91 mg, 5.00 μmol) in $CHCl_3$ (0.140 mL) was added a solution of cardiolipin sodium salt from bovine heart (CL, 1.86 mg, 1.25 μmol) in $CHCl_3$ (0.186 mL). The solution was concentrated, and dried under vacuum to form a lipid thin film. The thin film was hydrated and suspended in CF-containing buffer solution (0.250 mL, 5 mM HEPES, 20 mM CF, pH 7.5) by vortexing and sonication. After five-times freeze-thaw cycles, the lipid suspension was extruded 19 times through a polycarbonate filter with 0.40 μm of pore size in the diameter. The external CF-containing buffer was replaced with a CF-free buffer solution (20 mM HEPES, 1 mM EDTA, pH 7.5) through size exclusion chromatography using disposable PD-10 column. Concentration of EYPC was determined by using Phospholipid C-Test Wako. The final concentration of EYPC was adjusted to 4.0 μM with the CF-free buffer solution, and used for membrane disruption assay. Averaged molecular weight of CL (1489) was calculated from the reported data.[59]

*Preparation of CF-encapsulated LUVs consisting of PC/PG/MK or PC/PG/UQ.* To a solution of EYPC (9.48 mg, 12.4 μmol) and EYPG (9.66 mg, 12.4 μmol) in $CHCl_3$ (0.208 mL) was added a solution of **4** or **5** (0.313 μmol) in $CHCl_3$ (21.8 μL). The solution was concentrated, and dried under vacuum to form a lipid thin film. The thin film was hydrated and suspended in CF-containing buffer solution (0.500 mL, 5 mM HEPES, 20 mM CF, pH 7.5) by vortexing and sonication. After five-times freeze-thaw cycles, the lipid suspension was extruded 19 times through a polycarbonate filter with 0.40 μm of pore size in the diameter. The external CF-containing buffer was replaced with a CF-free buffer solution (20 mM HEPES, 1 mM EDTA, pH 7.5) through size exclusion chromatography using disposable PD-10 column. Concentration of EYPC was determined by using Phospholipid C-Test Wako. The final concentration of EYPC was adjusted to 4.0 μM with the CF-free buffer solution, and used for membrane disruption assay.

*Membrane disruption assay.* Peptides **1**-**3** were diluted with 40% aqueous MeOH to various concentrations as 5-fold serial dilutions. The solution of peptides (2 μL) and the CF-encapsulated LUV suspension (200 μL) were mixed in 96-well plates. The final concentration of peptides ranged from 2970 nM to 0.00152 nM. The 96-well plates were vortexed at rt for 30 min, and then fluorescence emission of each well was measured at 490 nm with the excitation at 517 nm using a fluorescence microplate reader. The LUV suspension and 5% aqueous Trion X-100 (2 μL) were mixed in each 96-well plate to determine 100% lysis. The LUV suspension and 40% aqueous MeOH (2 μL) and were mixed in each 96-well plate to determine 0% lysis. The membrane disruption activities of tested peptides ($I$) were normalized against 100% lysis ($I_{max}$) and 0% lysis ($I_0$) as following: $I = 100 \times (I_x - I_0)/ (I_{max} - I_0)$, where $I_x$ is the fluorescence intensity. The membrane-disrupting activities were evaluated as $EC_{50}$ (nM) by means of three replicates. Sigmoidal curve fittings were performed on R[60] with drc package (Figure S2).[61] Four-parameter logistic model was applied for the fitting. The obtained $EC_{50}$ values with S.D. (average of 3 independent experiments) were 503 ± 165 (PC/PG), 833 ± 68 (PC/PG/CL), 14.2 ± 3.1 (PC/PG/MK), and 132 ± 14 (PC/PG/UQ) nM for **1**, 640 ± 39 (PC/PG), 781 ± 54 (PC/PG/CL), 22.1 ± 12.9 (PC/PG/MK), and 261 ± 47 (PC/PG/UQ) nM for **2**, and 435 ± 83 (PC/PG), 501 ± 57 (PC/PG/CL), 15.9 ± 7.3 (PC/PG/MK), and 56.5 ± 11.9 (PC/PG/UQ) nM for **3**, respectively (Figure S3).

## ASSOCIATED CONTENT

**Supporting Information**. Determination of the configuration of **18**, chiral HPLC analysis of **19**, assay data, $^1$H and $^{13}$C NMR spectra for all new compounds, $^1$H-$^1$H COSY, $^1$H-$^1$H TOCSY, $^1$H-$^1$H NOESY, $^1$H-$^{13}$C HMBC, $^1$H-$^{13}$C HMQC spectra, and HPLC charts for peptides **1** and **2**. This material is available free of charge via the Internet at http://pubs.acs.org.

## AUTHOR INFORMATION

### Corresponding Author

*E-mail: inoue@mol.f.u-tokyo.ac.jp

### ORCID

Hiroaki Itoh: 0000-0002-1329-6109
Masayuki Inoue: 0000-0003-3274-551X

### Notes

The authors declare no competing financial interest.

## ACKNOWLEDGMENTS

This research was financially supported by Grant-in-Aids for Scientific Research (S) (JP17H06110) and Scientific Research on Innovative Areas (JP16H01130) to M.I., for Young Scientists (B) (JP17K15421) to H.I., Scientific Research (S) (JP15H05783) to K.S., and by Takeda Science Foundation to H.H. Fellowships from JSPS to T.K. and from Tokyo Biochemical Research Foundation to A.P. are gratefully acknowledged.

## REFERENCES

(1) Blair, J. M. A.; Webber, M. A.; Baylay, A. J.; Ogbolu, D. O.; Piddock, L. J. V. *Nat. Rev. Microbiol.* **2015**, *13*, 42.
(2) Brown, E. D.; Wright, G. D. *Nature* **2016**, *529*, 336.
(3) von Nussbaum, F.; Brands, M.; Hinzen, B.; Weigand, S.; Häbich, D. *Angew. Chem., Int. Ed.* **2006**, *45*, 5072.
(4) Butler, M. S.; Blaskovich, M. A.; Cooper, M. A. *J. Antibiot.* **2013**, *66*, 571.

(5) O'Connell, K. M. G.; Hodgkinson, J. T.; Sore, H. F.; Welch, M.; Salmond, G. P. C.; Spring, D. R. *Angew. Chem., Int. Ed.* **2013**, *52*, 10706.
(6) Wright, P. M.; Seiple, I. B.; Myers, A. G. *Angew. Chem., Int. Ed.* **2014**, *53*, 8840; *Angew. Chem.* **2014**, *126*, 8984.
(7) Schneider, T.; Müller, A.; Miess, H.; Gross, H. *Int. J. Med. Microbiol.* **2014**, *304*, 37.
(8) Harvey, A. L.; Edrada-Ebel, R.; Quinn, R. J. *Nat. Rev. Drug Discov.* **2015**, *14*, 111.
(9) Panthee, S.; Hamamoto, H.; Paudel, A.; Sekimizu, K. *Arch. Microbiol.* **2016**, *198*, 839.
(10) Wencewicz, T. A. *Bioorg. Med. Chem.* **2016**, *24*, 6227.
(11) Kato, A.; Nakaya, S.; Ohashi, Y.; Hirata, H.; Fujii, K.; Harada, K. *J. Am. Chem. Soc.* **1997**, *119*, 6680.
(12) Kato, A.; Nakaya, S.; Kokubo, N.; Aiba, Y.; Ohashi, Y.; Hirata, H. *J. Antibiot.* **1998**, *51*, 929.
(13) Kato, A.; Hirata, H.; Ohashi, Y.; Fujii, K.; Mori, K.; Harada, K. *J. Antibiot.* **2011**, *64*, 373.
(14) Zhang, W.; Li, Y.; Qian, G.; Wang, Y.; Chen, H.; Li, Y.-Z.; Liu, F.; Shen, Y.; Du, L. *Antimicrob. Agents Chemother.* **2011,** *55*, 5581.
(15) Wang, Y.; Qian, G.; Liu, F.; Li, Y.-Z.; Shen, Y.; Du, L. *ACS Synth. Biol.* **2013**, *2*, 670.
(16) Butler, M. S.; Cooper, M. A. *J. Antibiot.* **2011**, *64*, 413.
(17) Wohlrab, A. M. PhD thesis, University of California (2007).
(18) Hamamoto, H.; Urai, M.; Ishii, K.; Yasukawa, J.; Paudel, A.; Murai, M.; Kaji, T.; Kuranaga, T.; Hamase, K.; Katsu, T.; Su, J.; Adachi, T.; Uchida, R.; Tomoda, H.; Yamada, M.; Souma, M.; Kurihara, H.; Inoue, M.; Sekimizu, K. *Nat. Chem. Biol.* **2015**, *11*, 127.
(19) Panthee, S.; Hamamoto, H.; Suzuki, Y.; Sekimizu, K. *J. Antibiot.* **2017**, *70*, 204.
(20) Bentley, R.; Meganathan, R. *Microbiol. Rev.* **1982**, *46*, 241.
(21) Tynecka, Z.; Szcześniak, Z.; Malm, A.; Los, R. *Res. Microbiol.* **1999**, *150*, 555.
(22) Murai, M.; Kaji, T.; Kuranaga, T.; Hamamoto, H.; Sekimizu, K.; Inoue, M. *Angew. Chem., Int. Ed.* **2015**, *54*, 1556; *Angew. Chem.* **2015**, *127*, 1576.
(23) Kaji, T.; Murai, M.; Itoh, H.; Yasukawa, J.; Hamamoto, H.; Sekimizu, K.; Inoue, M. *Chem. Eur. J.* **2016**, *22*, 16912.
(24) Carpino, L. A.; Han, G. Y. *J. Am. Chem. Soc.* **1970**, *92*, 5748.
(25) Chan, W. C.; White, P. D. *Fmoc Solid Phase Peptide Synthesis—A Practical Approach* (Oxford Univ. Press, 2000).
(26) Garcia-Martin, F.; Quintanar-Audelo, M.; Garcia-Ramos, Y.; Cruz, L. J.; Gravel, C.; Furic, R.; Côte, S.; Tulla-Puche, J.; Albericio, F. *J. Comb. Chem.* **2006**, *8*, 213.
(27) Kates, S. A.; Solé, N. A.; Johnson, C. R.; Hudson, D.; Barany, G.; Albericio, F. *Tetrahedron Lett.* **1993**, *34*, 1549.
(28) Lee, J.; Griffin, J. H.; Nicas, T. I. *J. Org. Chem.* **1996**, *61*, 3983.
(29) Walther, T.; Arndt, H.-D.; Waldmann, H. *Org. Lett.* **2008**, *10*, 3199.
(30) Dixon, M. J.; Nathubhai, A.; Andersen, O. A.; van Aalten, D. M. F.; Eggleston, I. M. *Org. Biomol. Chem.* **2009**, *7*, 259.
(31) Pelay-Gimeno, M.; García-Ramos, Y.; Martin, M. J.; Spengler, J.; Molina-Guijarro, J. M.; Munt, S.; Francesch, A. M.; Cuevas, C.; Tulla-Puche, J.; Albericio, F. *Nat. Commun.* **2013**, *4*, 2352.
(32) Mazur, S.; Jayalekshmy, P. *J. Am. Chem. Soc.* **1979**, *101*, 677.
(33) White, C. J.; Yudin, A. K. *Nat. Chem.* **2011**, *3*, 509.
(34) Humphrey, J. M.; Chamberlin, A. R. *Chem. Rev.* **1997**, *97*, 2243.
(35) Stolze, S. C.; Kaiser, M. *Synthesis* **2012**, *44*, 1755.
(36) The TBS protection of D-OHAsn was important for increasing the overall yield of **1**.
(37) Itoh, H.; Matsuoka, S.; Kreir, M.; Inoue, M. *J. Am. Chem. Soc.* **2012**, *134*, 14011.
(38) Itoh, H.; Inoue, M. *Acc. Chem. Res.* **2013**, *46*, 1567.
(39) Noyori, R.; Ohkuma, T.; Kitamura, M.; Takaya, H.; Sayo, N.; Kumobayashi, H.; Akutagawa, S. *J. Am. Chem. Soc.* **1987**, *109*, 5856.
(40) Sang, F.; Ding, Y.; Wang, J.; Sun, B.; Sun, J.; Geng, Y.; Zhang, Z.; Ding, K.; Wu, L.-L.; Liu, J.-W.; Bai, C.; Yang, G.; Zhang, Q.; Li L.-Y.; Chen, Y. *J. Med. Chem.* **2016**, *59*, 1184.
(41) Boger, D. L.; Lee, R. J.; Bounaud, P.-Y.; Meier, P. *J. Org. Chem.* **2000**, *65*, 6770.
(42) Guzmán-Martínez, A.; VanNieuwenhze, M. *Synlett* **2007**, 1513.
(43) Yu, H.-M.; Chen, S.-T.; Wang, K.-T. *J. Org. Chem.* **1992**, *57*, 4781.
(44) Bacsa, B.; Horváti, K.; Bõsze, S.; Andreae, F.; Kappe, C. O. *J. Org. Chem.* **2008**, *73*, 7532.
(45) Carpino, L. A. *J. Am. Chem. Soc.* **1993**, *115*, 4397.
(46) Friedrich-Bochnitschek, S.; Waldmann, H.; Kunz, H. *J. Org. Chem.* **1989**, *54*, 751.
(47) Coste, J.; Le-Nguyen, D.; Castro, B. *Tetrahedron Lett.* **1990**, *31*, 205.
(48) Collins, M. D.; Jones, D. *J. Gen. Microbiol.* **1979**, *114*, 27.
(49) Wakeman, C. A.; Hammer, N. D.; Stauff, D. L.; Attia, A. S.; Anzaldi, L. L.; Dikalov, S. I.; Calcutt, M. W.; Skaar, E. P. *Mol. Microbiol.* **2012**, *86*, 1376.
(50) Sims, P. J.; Waggoner, A. S.; Wang, C.-H.; Hoffman, J. F. *Biochemistry* **1974**, *13*, 3315.
(51) Epand, R. M.; Epand, R. F. *Mol. BioSyst.* **2009**, 5, 580.
(52) Frerman, F. E.; White, D. C. *J. Bacteriol.* **1967**, *94*, 1868.
(53) Joyce, G. H.; Hammond, R. K.; White, D. C. *J. Bacteriol.* **1970**, *104*, 323.
(54) Weinstein, J. N.; Blumenthal, R.; Klausner, R. D. *Methods Enzymol.* **1986**, *128*, 657.
(55) Ohtani, I.; Kusumi, T.; Kashman, Y.; Kakisawa, H. *J. Am. Chem. Soc.* **1991**, *113*, 4092.
(56) Clinical and Laboratory Standards Institute. Methods for Dilution Antimicrobial Susceptibility Tests for Bacteria that Grow Aerobically; Approved Standard—Eighth Edition (CLSI document M07–A8) (Clinical and Laboratory Standards Institute, Wayne, PA, 2009).
(57) Clinical and Laboratory Standards Institute. Reference Method for Broth Dilution Antifungal Susceptibility Testing of Yeasts; Approved Standard (CLSI document M27-A) (Clinical and Laboratory Standards Institute, Wayne, PA, 1997).
(58) Breeuwer, P.; Abee, T. Assessment of the Membrane Potential, Intracellular pH and Respiration of Bacteria Employing Fluorescence Techniques (Kluwer Academic Publishers, Netherlands, 2004).
(59) Minkler, P. E.; Hoppel, C. L. *J. Lipid Res.* **2010**, *51*, 856.
(60) R Core Team (2016). R: A language and environment for statistical computing. R Foundation for Statistical Computing, Vienna, Austria. URL https://www.R-project.org/.
(61) Ritz, C.; Streibig, J. C. *J. Stat. Softw.* **2005**, *12*, DOI: 10.18637/jss.v012.i05.